iScience

CellPress

Article

A Unique Brain Connectome Fingerprint Predates and Predicts Response to Antidepressants

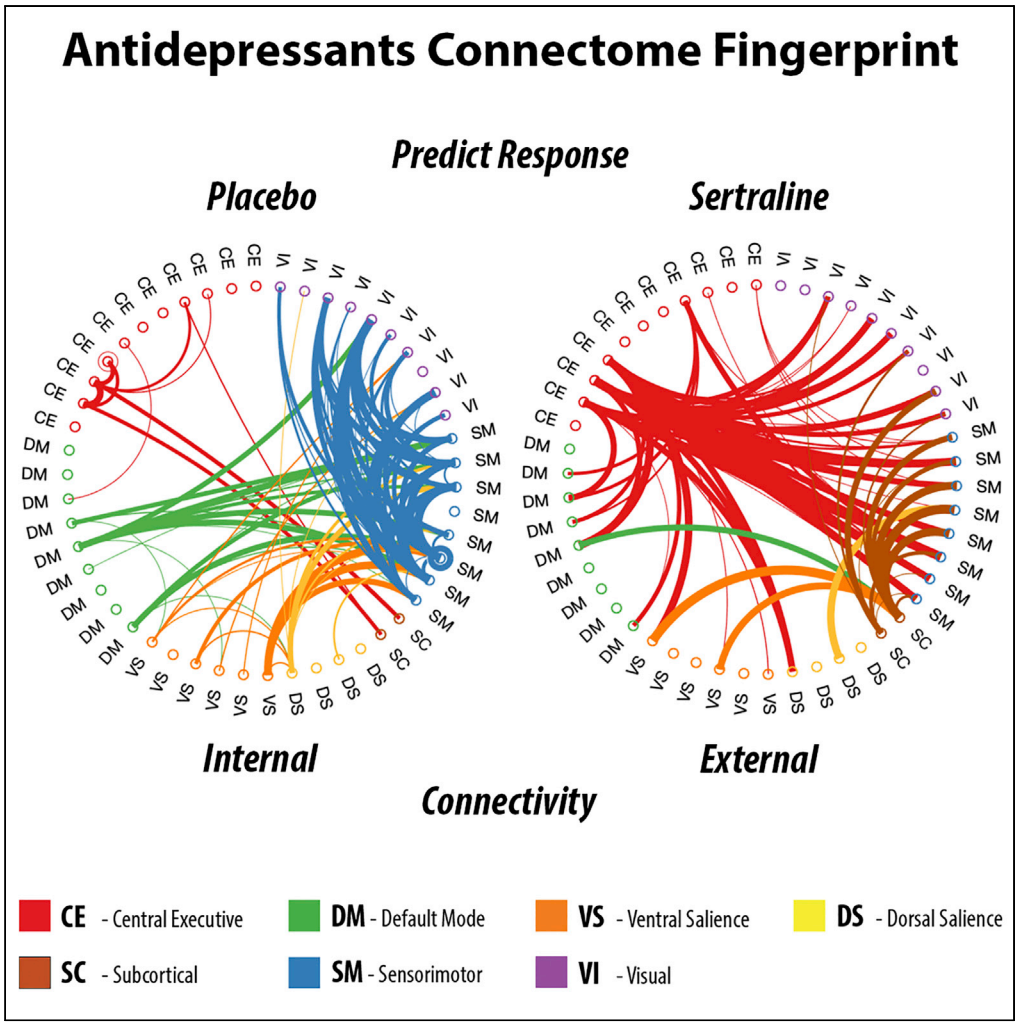

Samaneh Nemati, Teddy J. Akiki, Jeremy Roscoe, ..., J.F. William Deakin, Lynnette A. Averill, Chadi G. Abdallah

chadi.abdallah@yale.edu

HIGHLIGHTS

Machine learning methods were used to fully investigate the brain connectome

Network-informed features engineering approaches were proposed

A cortical-subcortical hierarchical brain atlas was established

A specific connectome signature was found to predict response to antidepressants

Nemati et al., iScience *23*, 100800
January 24, 2020
https://doi.org/10.1016/j.isci.2019.100800

iScience

CellPress

Article

A Unique Brain Connectome Fingerprint Predates and Predicts Response to Antidepressants

Samaneh Nemati,[1,2,6] Teddy J. Akiki,[1,2,6] Jeremy Roscoe,[1,2] Yumeng Ju,[2] Christopher L. Averill,[1,2] Samar Fouda,[1,2] Arpan Dutta,[3,4] Shane McKie,[3] John H. Krystal,[1,2] J.F. William Deakin,[3,5] Lynnette A. Averill,[1,2] and Chadi G. Abdallah[1,2,7,*]

SUMMARY

More than six decades have passed since the discovery of monoaminergic antidepressants. Yet, it remains a mystery why these drugs take weeks to months to achieve therapeutic effects, although their monoaminergic actions are present rapidly after treatment. In an attempt to solve this mystery, rather than studying the acute neurochemical effects of antidepressants, here we propose focusing on the early changes in the brain functional connectome using traditional statistics and machine learning approaches. Capitalizing on three independent datasets (n = 1,261) and recent developments in data and network science, we identified a specific connectome fingerprint that predates and predicts response to monoaminergic antidepressants. The discovered fingerprint appears to generalize to antidepressants with differing mechanism of action. We also established a consensus whole-brain hierarchical connectivity architecture and provided a set of model-based features engineering approaches suitable for identifying connectomic signatures of brain function in health and disease.

INTRODUCTION

The serendipitous discovery of slow acting antidepressants in the 1950s has generated persistent interest in identifying the biological underpinnings of depression and unraveling the mechanism of action of antidepressants (Ban, 2006). The clinical neuroscience field has since produced a wealth of knowledge related to the biological systems implicated in depression pathophysiology and to the neurochemical effects of these slow acting antidepressants, which tend to modulate monoaminergic neurotransmitters (Abdallah et al., 2018b; Coplan et al., 2014). Yet, despite more than six decades of research, it remains a mystery as to why the therapeutic behavioral effects of these drugs are only evident following weeks to months of treatment, whereas the neurochemical effects are acutely present after administration (Coplan et al., 2014). Solving this mystery may be critical to developing novel efficacious and rapid acting treatments for the large population of patients who are treatment resistant to currently available antidepressants (Trivedi et al., 2006). In recent years, accumulating evidence implicated brain circuitry and functionally connected networks in the pathology and treatment of depression (Kaiser et al., 2015). Hence, rather than focusing on the acute synaptic neurochemical effects of monoaminergic antidepressants, it may be more revealing to examine the role of early brain network changes in the mechanisms of these slow acting antidepressants.

A consistent evidence in the field is that the behavioral severity of depression significantly improves following placebo treatment, at times leading to lack of behavioral difference between placebo treatment and well-established antidepressants (Andrews, 2001). The placebo response could be due to nonspecific effects or to the milieu effects of research studies (e.g., repeated visits and assessments). Although the placebo effect is a major impediment for efficacy studies, we here used the significant improvement in depression following placebo to our advantage, as it provided an optimal control for both the test-retest of fMRI and depression measures, as well as controlling for behavioral improvement due to nonspecific and milieu effects. This allowed us to identify the biological correlates of response to the studied antidepressants, controlling for test-retest and nonspecific response. Focusing on the interaction between treatment and response, we implemented data-driven approaches to test three hypotheses.

[1]National Center for PTSD – Clinical Neuroscience Division, US Department of Veterans Affairs, 950 Campbell Avenue 151 E, West Haven, CT 06516, USA

[2]Department of Psychiatry, Yale University School of Medicine, New Haven, CT, USA

[3]University of Manchester, Manchester, UK

[4]Mersey Care NHS Foundation Trust, Liverpool, UK

[5]Greater Manchester Mental Health NHS Foundation Trust, Manchester, UK

[6]These authors contributed equally

[7]Lead Contact

*Correspondence: chadi.abdallah@yale.edu

https://doi.org/10.1016/j.isci.2019.100800

Hypothesis 1—Better Response to Sertraline Would Be Predicted by an Increase in Prefrontal Cortex and Caudate Global Brain Connectivity

Global brain connectivity (GBC) is a measure of nodal strength within a network. Nodal strength is the most fundamental measure in a graph, as most other topology measures are affected by or are partially derived from nodal strength (Bullmore and Sporns, 2009). GBC is calculated as the average connectivity between a node (e.g., a gray matter voxel) and all other nodes within a network (e.g., all gray matter voxels) (Cole et al., 2011). In major depressive disorder (MDD), widespread reduction in GBC and other comparable nodal strength measures has been repeatedly demonstrated across samples and by several research groups, particularly in regions within the prefrontal cortex (PFC) (Abdallah et al., 2017a, 2017b; Holmes et al., 2019; Murrough et al., 2016; Scheinost et al., 2018; Wang et al., 2014). Moreover, increased GBC in bilateral caudate or lateral PFC following or during infusion with the rapid acting antidepressant ketamine was associated with enhanced response (Abdallah et al., 2017b, 2018a). Compared with healthy controls, patients with MDD were also found to have high GBC in the posterior cingulate, a critical node within the default mode (DM) network (Abdallah et al., 2017b). This DM GBC dysconnectivity is also normalized following ketamine treatment (Abdallah et al., 2017b). The GBC approach has two essential strengths: (1) nodal strength is a fundamental topology measure within a network, and (2) whole-brain analysis can be conducted, without the limitation and the bias of a priori seed selection. However, a main limitation of GBC is the inability to determine which edges (i.e., connection between two regions) are driving the abnormalities. This limitation is addressed in the current study by the use of network-restricted strength (NRS) and NRS predictive model (NRS-PM) approaches, described in hypotheses 2 and 3. Another limitation of GBC is that it does not capture network changes in opposing directions, e.g., a balanced dynamic network shift from internal to external connectivity cannot be captured using GBC values. To address this issue, we here implemented two measures: nodal internal NRS (niNRS) and nodal external NRS (neNRS).

Hypothesis 2—Better Response to Sertraline Would Be Predicted by a Reduction in Internal Default Mode Network-Restricted Strength

The DM comprises brain regions that are synchronously activated at rest and deactivated during external tasks (Andrews-Hanna et al., 2014). Although not without inconsistency (Mulders et al., 2015; Sexton et al., 2012), seed based, independent component, and meta-analysis results have suggested DM hyperconnectivity in MDD compared with controls (Alexopoulos et al., 2012; Greicius et al., 2007; Kaiser et al., 2015; Sheline et al., 2010; Wu et al., 2011). To date, connectivity studies have primarily used seed-based approaches to identify abnormalities or changes in DM of patients with MDD. Among the limitations of this approach are (1) one (or a few) seeds do not cover all the nodes of the DM and the target clusters, hence potentially lowering sensitivity and complicating interpretability of the findings, and (2) it would be difficult to fully integrate findings across studies as they are often highly dependent on the seed location (Akiki et al., 2018). Alternatively, whole-brain topology measures address some of these limitations but fail to identify the specific interactions within and between networks (a.k.a., modules, systems, or communities; e.g., DM).

Borrowing from studies of complex systems (Gu et al., 2015; Guimera and Amaral, 2005), NRS approaches address these limitations and have been successfully implemented in the study of psychopathology (Akiki et al., 2018; Etkin et al., 2019; Nusslock et al., 2019; Schultz et al., 2018; Yang et al., 2018). Briefly, the network-restricted approach used in this study is capable of comprehensively assessing all identifiable nodes in a given brain network (e.g., DM), to extract internal connectivity strength within that network and also calculate the external connectivity between networks. To ensure reproducibility in future studies, we opted to use a consensus hierarchical modularity atlas recently established in 1,003 subjects with high-quality functional magnetic resonance imaging (fMRI) data (Akiki and Abdallah, 2019). Based on the hypothesized hyperconnectivity in DM, we investigated whether reduction in internal DM connectivity would predict better response to sertraline. This was followed by exploratory analysis, with appropriate correction for multiple comparisons, to determine whether response to sertraline is predicted by connectivity within or between brain networks.

Hypothesis 3—Better Response to Sertraline Would Be Predicted by a Consensus-Based NRS Predictive Model

Machine learning methods have been increasingly implemented in the study of psychopathology (Galatzer-Levy et al., 2018). Among the strengths of machine learning algorithms are the fully data-driven approach and the cross-validation component often included in these predictive models, which could address the issue of over-fitting in interpretive models (e.g., regression) and may enhance generalizability

to new data (Scheinost et al., 2019; Shen et al., 2017). However, these machine learning approaches have two critical limitations in the study of psychopathology: (1) They are faced with large number of features (e.g., there are 1,799,970,000 unique edges in a cifti-based fMRI dense connectome) compared with the number of observations, which in psychiatry are often in the order of dozens to hundreds. (2) Considering the dimensionality reduction and weighting procedures involved, it is often not possible to back translate the selected/weighted features to the original space to visualize and understand the underlying neurobiology (Shen et al., 2017). Connectome-based predictive model (CPM) is a linear machine learning approach, which retains the ability to back translate findings to the original feature space (Finn et al., 2015; Shen et al., 2017). However, a limitation of CPM is the use of individual parcellated nodes, which leads to a relatively high number of features (e.g., there are 89,676 unique edges in the A424 atlas), which subsequently complicates the interpretability of the findings as the edges included in the final model are often in the order of thousands. Moreover, these nodes are based on anatomical location rather than on network affiliations. To address these limitations, we implemented an NRS-PM that reduces the connectome input features and facilitates the neurobiological interpretation of the final model, as all input features are network based. To assess the robustness of the approach and to rule out potential bias related to architecture selection, we investigated NRS-PM across all architecture levels—with and without subcortical structures, we deconstructed GBC into nodal internal and external NRS, and we determined the full connectome (FC-PM) results using a whole-brain multimodal atlas with 424 nodes (i.e., A424).

Overall, we aimed to determine whether early changes in brain functional connectivity predates and predicts response to slow acting antidepressants. To answer this question, we analyzed publicly available data from a relatively large neuroimaging clinical trial in which depressed patients (n = 202) were randomized to placebo or sertraline, a typical monoaminergic slow acting antidepressant (Trivedi et al., 2016). We then leveraged a large dataset of high-quality fMRI from healthy volunteers (n = 1,003) who participated in the Human Connectome Project (Van Essen et al., 2013) to establish a whole-brain hierarchical parcellation of intrinsic connectivity networks (ICNs). The latter allowed us to extend the cortical findings to subcortical and cerebellar brain regions. Finally, encouraged by the predictive model findings, we conducted a pilot analysis to determine whether the identified connectomic signature related to sertraline response could predate and predict response to the rapid acting antidepressant ketamine, compared with both active and inactive control (Abdallah et al., 2018a; Downey et al., 2016).

RESULTS

The sertraline dataset was acquired from the National Institute of Mental Health Data Archive (NDA), Establishing Moderators and Biosignatures of Antidepressant Response for Clinical Care (EMBARC). All participants (n = 202) with successful resting state fMRI at baseline and week 1, who completed depression assessment at week 8, were included in the current study. The protocol and results of the EMBARC clinical trial were reported elsewhere (Pizzagalli et al., 2018; Trivedi et al., 2006). Briefly, unmedicated patients with chronic or recurrent MDD were randomized to 8 weeks of daily oral placebo or sertraline. Demographics and clinical features are described in Table 1. Hamilton rating scale for depression (HAMD) was used to determine severity. Response was defined as at least 50% improvement in HAMD at week 8, the time point at which full clinical benefit is expected following slow acting antidepressant treatment.

The Antidepressant Response Is Associated with Early Increase in Caudate Global Connectivity

Guided by previous work with antidepressants (Abdallah et al., 2017b), we first conducted a whole-brain vertex-/voxel-wise GBC analysis, with false discovery rate (FDR) correction ($q < 0.05$), examining the interaction between treatment (sertraline versus placebo) and response (responders versus non-responders). We found that increased GBC in bilateral caudate and right rostral anterior cingulate (rACC) at week 1 were associated with better response to sertraline at week 8 compared with placebo (Figure 1A). Two clusters with reduced GBC in left Brodmann areas 4 (motor) and 5 (somatosensory) were associated with better response to sertraline (Figure 1A). The independent effects of response and treatment are provided in the Supplemental Information (Figure S1).

These results confirmed the predicted role of caudate GBC but failed to show an association between antidepressant response and increased lateral PFC GBC (hypothesis 1). We speculated that this failure may be due to the limitations (see Supplemental Information) of the vertex-/voxel-wise interpretive analysis. To rule out this possibility, we implemented a nodal strength predictive model (nS-PM), with 1,000 iterations of

Characteristics	Sertraline (n = 99)	Placebo (n = 103)
Demographic		
Age, mean (SD)	38.5 (14.2)	37.1 (12.2)
Male	30.3%	35.9%
Years of education, mean (SD)	15.2 (2.6)	15.2 (2.4)
Clinical features		
Age of onset, mean (SD)	13.6 (5.4)	14.3 (5.5)
Chronic	55%	50%
Baseline HAMD, mean (SD)	18.9 (4.4)	18.5 (4.3)
W1 HAMD, mean (SD)	16.1(5.5)	15.8(5.1)
W8 HAMD, mean (SD)	11.1(6.5)	11.8(7.3)
W1 response	9%	7%
W8 response	47%	35%[a]

Table 1. Demographics and Clinical Characteristics

W1, week 1; W8, week 8; HAMD, Hamilton Rating Scale for Depression.

[a]There were no significant ($p > 0.1$) differences between treatment groups, except for response rate at week 8, which showed a trend (chi square = 2.8, $p = 0.096$).

10 cross-validation (*CV*), to identify brain regions that significantly predict a continuous measure of improvement following sertraline compared with placebo. Changes in nodal GBC (i.e., nS) at week 1 significantly predicted improvement at week 8 following sertraline compared with placebo ($r = 0.23$, $CV = 10$, *iterations* = 1,000, $p \leq 0.001$). Enhanced antidepressant response was associated with increased nodal GBC in bilateral caudate and left lateral PFC, along with other brain regions primarily located within the central executive (CE) ICN (Figure 1B). Reduced nodal GBC in several regions within the visual (VI) and sensorimotor (SM) ICNs also predicted better antidepressant response, compared with placebo (Figure 1B).

Early Reduction in Default Mode Connectivity Predates the Antidepressant Response

Employing validated NRS methods (Akiki et al., 2018), we constructed a general linear model examining the effects of treatment, response, and treatment-by-response on changes in internal DM NRS (i.e., week 1 minus pretreatment). We found a significant treatment-by-response interaction ($F_{(1,195)} = 5.0$, $p = 0.026$), such that, compared with placebo, reduction in DM NRS at week 1 predicted better response to sertraline at week 8. There were no significant response or treatment effects ($p > 0.1$).

These results confirmed the predictions of hypothesis 2. Yet, to better characterize the DM findings and inform future studies, we conducted a follow-up analysis, with FDR correction, examining internal and external connectivity of all cortical ICNs (Figure 2A, i.e., DM, CE, dorsal salience [DS], ventral salience [VS], SM, and VI). Following correction for multiple comparisons, there was significant treatment-by-response interactive effect on the CE-SM edge ($F_{(1,195)} = 10.4$, $p = 0.001$), reflecting increased connectivity predicts better response to sertraline compared with placebo. There was also significant treatment effect on the CE-SM edge ($F_{(1,195)} = 11.0$, $p = 0.001$), reflecting increased connectivity at week 1 following sertraline, compared with placebo (Figure S2). There were no other significant treatment, response, or treatment-by-response effects ($q > 0.05$).

The Whole-Brain Hierarchical Atlas Reveals the Subcortical Affiliation of GBC Findings

To identify the ICN affiliation of the subcortical GBC findings and to extend the cortical NRS to subcortical and cerebellar regions, we next aimed to determine the hierarchical architecture of the whole brain using

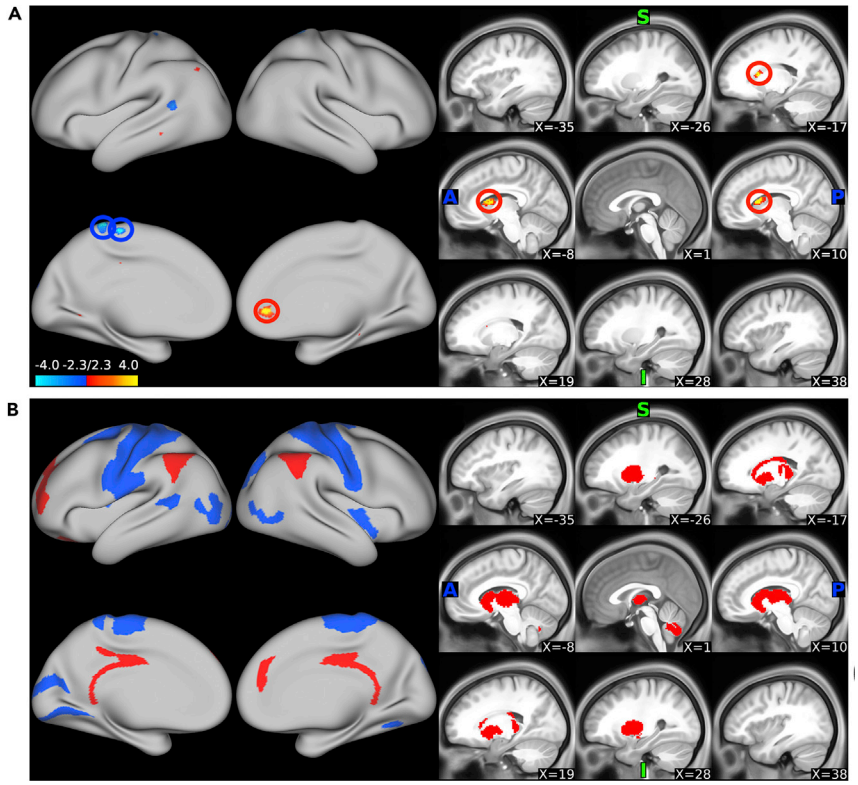

Figure 1. Early Global Functional Connectivity Changes Predict Response to Sertraline

(A) Whole-brain interpretive analysis showed a significant interaction between treatment and response, such that increased global brain connectivity (GBC) in the bilateral caudate and right rostral anterior cingulate (red circles) and decreased GBC in sensorimotor cortices (blue circles) at week 1 predicted response to sertraline at week 8 post treatment. The color bar represents the *z* values (threshold at $p < 0.005$, with circles denoting clusters that survived FDR correction at $q < 0.05$).

(B) Nodal strength (nS; i.e., nodal GBC) predictive model analysis ($p \leq 0.001$) revealed widespread nS increase in central executive and higher order association areas (red clusters) and decrease in nS within primary cortices (e.g., sensory, motor, and visual; blue clusters) at week 1 as predictors of enhanced response to sertraline at week 8, compared with placebo.

subject-level clustering of functional networks from 1,003 adult healthy subjects (Van Essen et al., 2013). Using consistent definition of community across cortical, subcortical, and cerebellar structures, the whole-brain subject-level clustering and consensus community detection algorithm identified 136 significant architecture (Figures 3 and S3). The hierarchical atlas, here termed Akiki-Abdallah (AA) atlas, delineated architectures ranging from 3 to 150 modules. The cortical modules remained largely consistent with the cortex-only atlases in our previous work (Akiki and Abdallah, 2019) and in the literature (Yeo et al., 2011), as shown in Figures 2A versus 2C. The AA architecture at 24 modules (AA-24) largely matches the cortical 22 modules architecture (see Supplemental Information and Figure S4) while adding the affiliation of subcortical and cerebellar nodes. AA-50 is the architecture with the highest similarity to subject-specific modularity (Figures 3B and S3D). Notably, the ICN affiliations of the positive predictive GBC nodes findings were within the CE and global-pallidus-putamen subcortical (GPu SC) modules, whereas the negative predictive GBC nodes were within the SM and VI networks (see Figures 1B versus 3C).

A Connectome Fingerprint Predates and Predicts Enhanced Antidepressant Response

Following ICN hierarchical parcellation, we aimed to determine whether a whole-brain connectome fingerprint predates and predicts response to sertraline, compared with placebo. As shown in Figure S5B, the whole-brain NRS-PM predicted the antidepressant response across AA-4 to AA-150 architectures (following FDR correction), with a peak at AA-58 ($r = 0.27$, $CV = 10$, *iterations* = 1,000, $p = 0.003$). Independently, the positive predictive edges peaked at AA-58 ($r = 0.29$, $CV = 10$, *iterations* = 1,000, $p = 0.001$) and

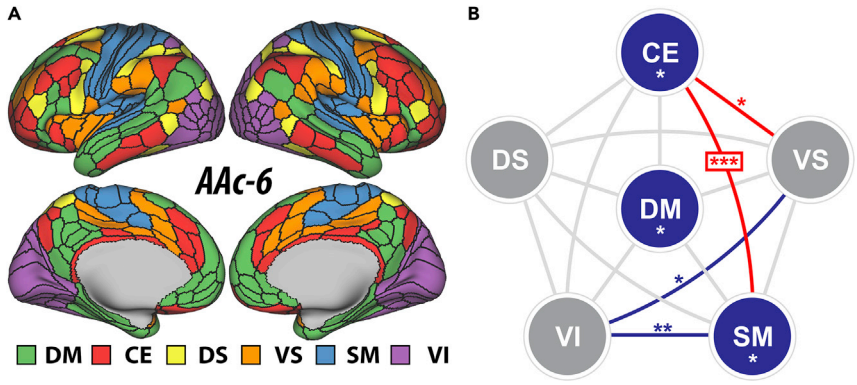

Figure 2. Early Changes in Network-Restricted Connectivity Predict Response to Sertraline

(A) The networks nodal affiliation based on the Akiki-Abdallah cortical (AAc) hierarchical atlas at 6 modules (AAc-6) (Akiki and Abdallah, 2019), which includes the default mode (DM), central executive (CE), dorsal salience (DS), ventral salience (VS), sensorimotor (SM), and visual (VI) networks.

(B) The network-restricted strength (NRS) pentagon. Internal NRS is depicted as filled circles, whereas inter-networks external NRS is depicted as edges. * was used for $p < 0.05$, ** for $p < 0.01$, *** for $p < 0.001$. Interactions that survived FDR correction were denoted with squares (i.e., CE-SM edge). Filled circles and edges were colored gray for non-significant effects, blue for negative effects, and red for positive effects. The NRS interpretive analysis examining the interactive effects between treatment and response showed significant increase in connectivity between CE and SM at week 1 that predicts response to sertraline at week 8. This figure was adapted with permission from the Emerge Research Program (http://emerge.care).

the negative predictive edges peaked at AA-26 ($r = 0.25$, $CV = 10$, *iterations* = 1,000, $p = 0.003$). Compared with cortical NRS-PM, the inclusion of subcortical structure appears to have enhanced models, particularly positive predictions that were more consistent in independently predicting antidepressant response across architectures (Figure S5).

To further assess the whole-brain NRS-PM results, the AA-24 and AA-50 were visualized in Figures 4A and 4B, respectively. Predictive edges were comparable with findings with cortical atlas (see Supplemental Information and Figure S4), with richer connectomic signature and two highlights: (1) Modules within the CE and GPu SC ICNs showed reduced internal connectivity among each other but increased connectivity to the rest of the brain as predictors of enhanced antidepressant response. (2) Reduction in internal connectivity within the remaining ICNs, particularly SM and VI, also predicted better sertraline response. Modules containing the amygdala and insula also showed a shift from connection with primary cortices (e.g., sensory, motor, and visual) to increased connectivity with higher order association areas (Figure 4).

The Full Connectome Predicts Response but Yields Undiscernible Connectomic Signature

We next investigated whether a nodal based (i.e., 424x424 nodes) full connectome PM (FC-PM) would yield comparable or differing results, compared with whole-brain NRS-PM. The FC-PM significantly predicted the antidepressant response ($r = 0.27$, $CV = 10$, *iterations* = 1,000, $p = 0.005$). However, considering the large number of predictive edges, visualizing the PM is unable to discern the underlying connectomic signature (Figure 4C). Retaining the nodes with the highest degree (i.e., top 2.5% of each of positive and negative predictive edges) showed a pattern of reduced internal connectivity among nodes in the SM and VI network, but at the expense of discarding 95% of the model, and failed to reveal the internal-to-external shift within the CE network (Figure 4D).

Quantifying a Clinically Relevant Internal to External Connectivity Shift

Together, the network-restricted interpretative and predictive results supported the nS-PM GBC findings of increased connectivity in nodes within the CE and GPu SC but reduced connectivity in the SM and VI networks as predictor of response (Figures 1, 2, 3, and 4). However, the CE shift from internal to external connectivity cannot be captured by GBC measures, as the latter is an average of both internal and external connectivity. Therefore, to quantify the NRS shift, we deconstructed nS (i.e., nodal GBC) into two complementary measures: (1) nodal internal NRS (niNRS) calculated as the average connectivity between each node and all other nodes within the same ICN and (2) nodal external NRS (neNRS) calculated as the average

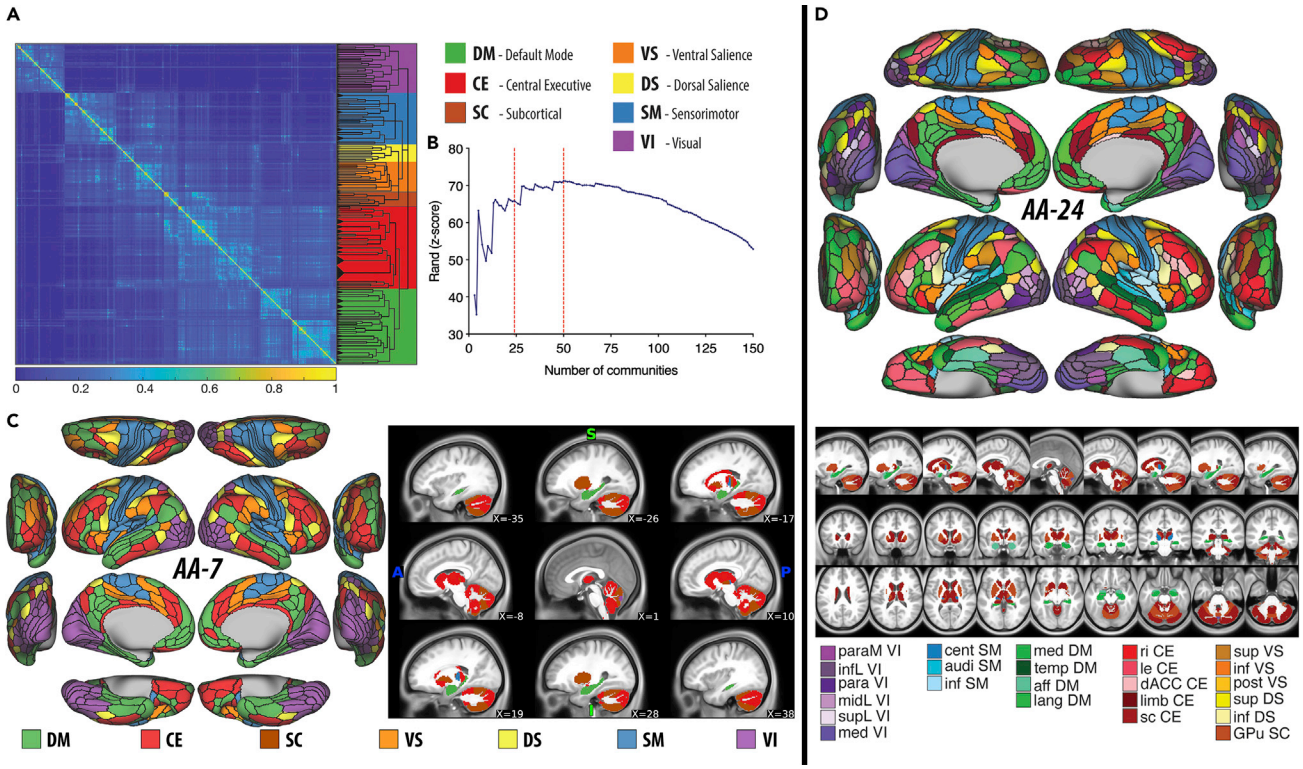

Figure 3. Whole-Brain Hierarchical Brain Architecture of Functional Connectivity Networks

(A) Co-classification matrix summarizing the results of the whole-brain clustering atlas in 1,003 healthy subjects, here termed Akiki-Abdallah (AA) atlas. The dendrogram represents the hierarchical organization of the nested communities. The background colors represent the network affiliation at 7 modules architecture (i.e., AA-7).

(B) Similarity plot showing the mean similarity between the partitioning in each consensus hierarchical level (i.e., from AA-3 to AA-150) and the subject-level clustering quantified by *Z* score of the Rand coefficient (blue line); the Rand score peaked at AA-50. The dashed red lines denote the brain architecture levels for Figures 3D and S3D.

(C and D) These maps show the whole-brain networks nodal affiliation at AA-7 (corresponds to the six main cortical networks) and AA-24 (corresponds to the peak subject-level similarity in the cortical atlas). The module abbreviations of AA-24, along with further details about the affiliation of each node, are reported in Table S1. The figures were adapted with permission from the Emerge Research Program (http://emerge.care). The hierarchical atlas maps and codes will be made publicly available at https://github.com/emergelab.

connectivity between each node and all other nodes outside its ICN. Here, we used AA-7, which comprises the main brain networks while incorporating subcortical structures, including CE, DM, VS, DS, SC, SM, and VI networks (Figure 3C). Changes in neNRS at week 1 significantly predicted improvement at week 8 following sertraline treatment compared with placebo (r = 0.28, CV = 10, $iterations$ = 1,000, $p \leq 0.001$). Enhanced antidepressant response was associated with increased neNRS in brain regions primarily located within the CE and GPu SC networks (Figures 5A and 5B). Similarly, changes in niNRS significantly predicted the antidepressant response (r = 0.24, CV = 10, $iterations$ = 1,000, p = 0.005). Enhanced antidepressant response was associated with reduced niNRS in brain regions primarily located within the CE, GPu SC, SM, and VI networks (Figures 5C and 5D). These results quantitatively demonstrated the internal-to-external NRS shift as predictor of antidepressant response. The cortical and whole-brain neNRS-PMs and niNRS-PMs across all architectures are provided in Supplemental Information (Figures S6 and S7). Similar to the NRS-PMs, including subcortical structures resulted in more consistent neNRS-PMs and niNRS-PMs across architectures (Figures S6 and S7).

The Predictive Models Partially Generalize to the Rapid Acting Antidepressant Ketamine

Encouraged by the robust NRS-PM findings, we conducted a pilot follow-up analysis to investigate the generalizability of the identified whole-brain models in predicting the antidepressant response to ketamine, a well-established rapid acting antidepressant (Abdallah et al., 2018b). Here, we used data from a previously published pharmacoimaging study, which examined brain functional connectivity at a period that predates

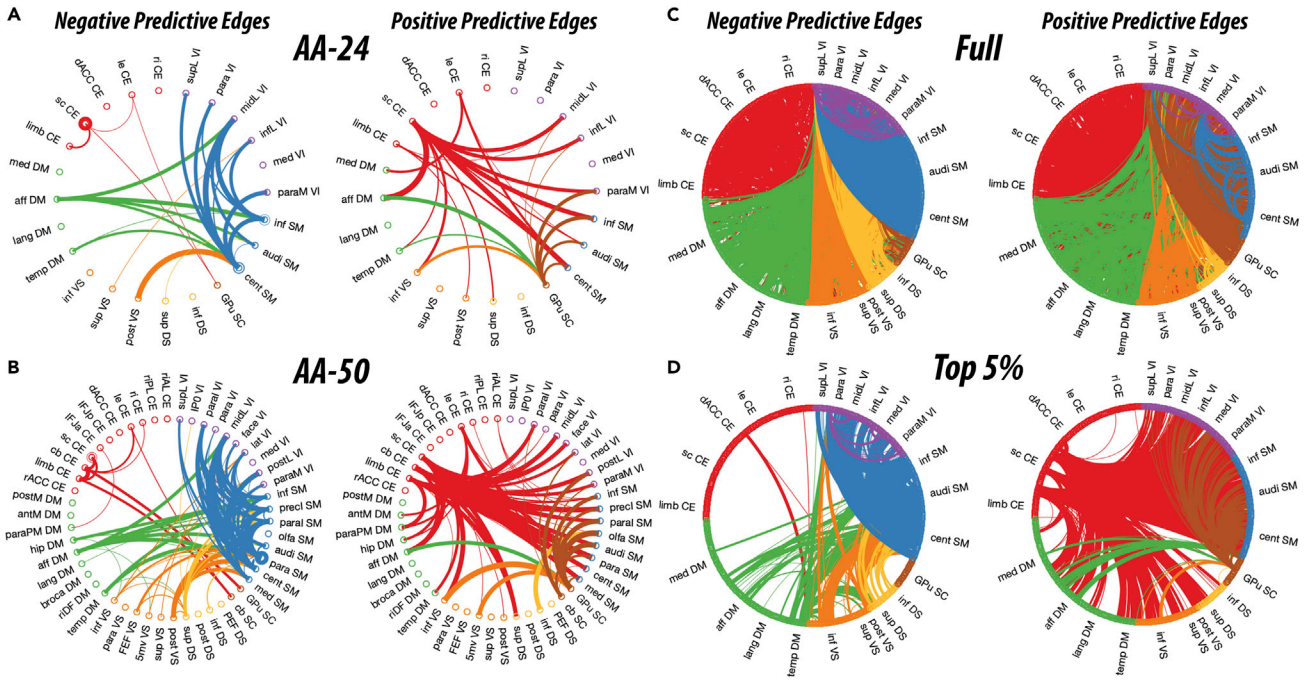

Figure 4. A Unique Brain Functional Connectome Fingerprint Predates and Predicts Response to Sertraline

(A and B) Network-restricted strength (NRS) predictive models (NRS-PMs; p = 0.032 and p = 0.033, respectively) revealed a specific connectomic signature evident at week 1 post treatment, at a time of no clinically meaningful antidepressant effects, that predicts enhanced response to sertraline at week 8, compared with placebo. An overall pattern emerged consistent of reduced connectivity between modules within the central executive (CE) and globus-pallidus-putamen subcortical (GPu SC) networks, along with increased connectivity between these two networks (CE/GPu SC) and the rest of the brain as predictors of enhanced response to sertraline. The connectome fingerprint (CFP) also showed reduction in internal connectivity within the visual and sensorimotor networks, as well as reduced interference on these two networks from modules within the default mode and salience networks.

(C) The full connectome predictive model (FC-PM; p = 0.005) predicted response to sertraline, but it was not possible to visually discern the underlying signature considering the large number of edges retained in the PM.

(D) Using nodal strength within the FC-PM as cutoff to retain the highest top 2.5% negative predictive edges and top 2.5% positive predictive edges showed a pattern consistent with the NRS-PM findings, but at the expense of discarding 95% of the data, and did not fully depict the shift from internal to external strength within the CE and GPu SC networks. ***Notes***: The circular graphs in 4A, 4C, and 4D are labeled based on the Akiki-Abdallah (AA) whole-brain architecture at 24 modules (AA-24; see Figure 3D; Table S1), whereas 4B is based on AA-50 (see Figure S3D; Table S1). Modules are colored according to their AA-7 network affiliation (see Figure 3C). Edges are colored based on the initiating module using a counter-clockwise path starting at 12 o'clock. Internal edges (i.e., within module NRS) are depicted as outer circles around the corresponding module. Thickness of edges reflects their corresponding weight in the predictive model. The module abbreviations of AA-24 and AA-50, along with further details about the affiliation of each node, are reported in Table S1. The predictive models will be made publicly available at https://github.com/emergelab.

the antidepressant effects of ketamine (i.e., during infusion) (Abdallah et al., 2018a; Downey et al., 2016). In this study, 56 patients with MDD were randomized to ketamine, lanicemine, or normal saline. The antidepressant effects of ketamine often arise within hours of its administration. Thus, we examined whether connectivity changes during ketamine infusion predates and predicts response at 24h post treatment, using lanicemine and normal saline as active and inactive control arms, respectively. Ketamine and lanicemine are both *N*-methyl-D-aspartate (NMDA) receptor antagonists; therefore, the lanicemine arm provided control for both the milieu effect (assessments, infusion, scans, etc.) as well as the acute non-specific NMDA modulation of connectivity networks during infusion (Abdallah et al., 2018a; Downey et al., 2016).

Following FDR correction for multiple comparisons, the three whole-brain predictive models established in the sertraline study—here termed sertraline connectome fingerprint (CFP)—predicted ketamine response compared with lanicemine at AA-24-CFP (r = 0.52, n = 38, p = 0.0008), AA-50-CFP (r = 0.57, n = 38, p = 0.0002) and full connectome FC-CFP (r = 0.55, n = 38, p = 0.0003). All three sertraline CFPs failed to predict ketamine response, compared with placebo (p > 0.05).

To further characterize the ketamine versus lanicemine findings, we conducted whole-brain NRS-PM at AA-24 and AA-50, as well as FC-PM. All three models significantly predicted treatment response to

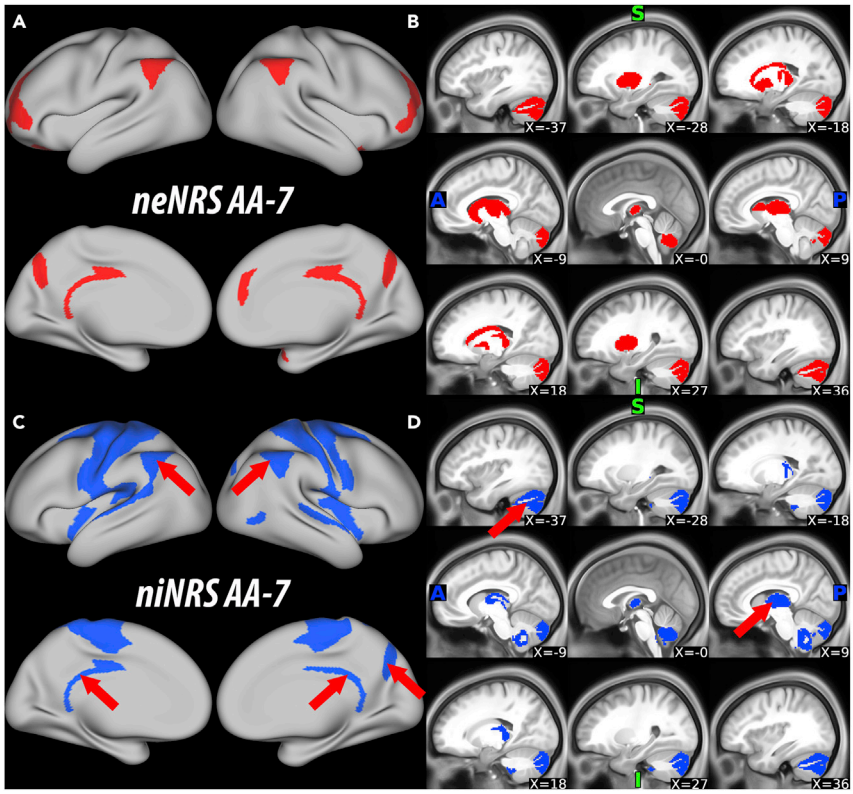

Figure 5. Quantifying the Internal to External Connectivity Shift

(A and B) A predictive model ($p \leq 0.001$) using nodal external network-restricted strength (neNRS) as input, based on Akiki-Abdallah (AA) whole-brain atlas at the architecture with 7 modules (AA-7), predicted enhanced response to sertraline. The model showed increased global external connectivity in brain regions within the central executive (CE) and globus-pallidus-putamen subcortical (GPu SC) networks. There were no reductions in global external connectivity.

(C and D) A predictive model ($p = 0.005$) using nodal internal network-restricted strength (niNRS) as input, based on AA-7, predicted enhanced response to sertraline. The model showed reduced internal connectivity in brain regions within the CE, GPu SC, sensorimotor, and visual networks. There were no increases in internal connectivity. Red arrows point to regions that showed both reduced niNRS and increase neNRS, all of which located within the CE and GPu SC networks, consistent with the internal-to-external connectivity shift observed in previous analyses and quantitively supporting the observed pattern of a shift toward increased higher order control over primary cortices.

ketamine, compared with lanicemine ($r = 0.41$ to 0.48, $CV = 10$, *iterations* = 1,000, $p < 0.05$). As shown in Figure 6, the identified models were largely comparable with those found in the sertraline versus placebo results.

DISCUSSION

Using a set of traditional statistics and machine learning approaches, the study results provided strong evidence of a specific connectome fingerprint (CFP) that predates and predicts response to the slow acting antidepressant, sertraline. The study established a whole-brain hierarchical ICNs atlas and provided evidence of its relevance to the study of psychopathology and to clinical neuroscience discovery. It also presented specialized measures and tested the robustness of innovative approaches, i.e., NRS-PM, niNRS-PM, and neNRS-PM. The impact of these atlases, measures, and approaches is expected to go beyond the current findings, as similar approaches could be used to identify the CFPs of various brain functions in health and disease. Finally, the study provided pilot evidence about the potential generalizability, albeit at a much shorter timescale, of the identified CFP to the mechanisms of rapid acting antidepressants.

Partially supporting hypothesis 1, bilateral caudate clusters of increased global connectivity at week 1 post treatment predicted better response to sertraline compared with placebo at week 8 (Figure 1A). Treatment response was also associated with decreased global connectivity in the sensory motor area but increased

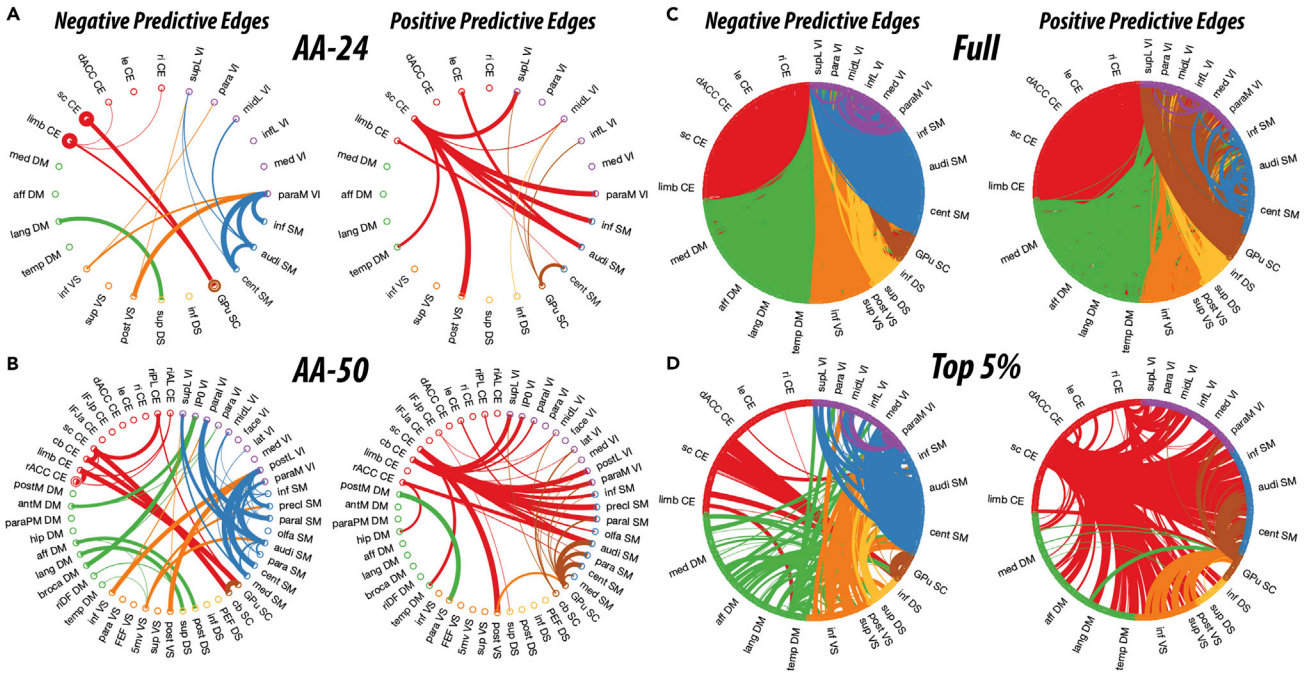

Figure 6. A Comparable Brain Functional Connectome Signature Predates and Predicts Response to Ketamine

(A and B) Network-restricted strength (NRS) predictive models (NRS-PMs; p = 0.003 and p = 0.002, respectively) revealed a comparable connectome fingerprint evident at 20 min during infusion, which predicts enhanced response to ketamine at 24 h, compared with active control. The overall pattern is consistent with findings in the sertraline models (Figure 4), but at a significantly shorter scale (i.e., at 20 min compared with at 7 days).

(C) The full connectome predictive model (FC-PM) predicted response to ketamine compared with active control, but it was not possible to visually discern the underlying signature considering the large number of edges retained in the PM.

(D) Using nodal strength within the FC-PM as cutoff to retain the highest top 2.5% negative predictive edges and top 2.5% positive predictive edges showed a pattern consistent with the NRS-PM findings, but at the expense of discarding 95% of the data. ***Notes***: The circular graphs in 6A, 6C, and 6D are labeled based on the Akiki-Abdallah (AA) whole-brain architecture at 24 modules (AA-24; see Figure 3D; Table S1), whereas 6B is based on AA-50 (see Figure S3D; Table S1). Modules are colored according to their AA-7 network affiliation (see Figure 3C). Edges are colored based on the initiating module using a counter-clockwise path starting at 12 o'clock. Internal edges (i.e., within module NRS) are depicted as outer circles around the corresponding module. Thickness of edges reflect their corresponding weight in the predictive model. The module abbreviations of AA-24 and AA-50, along with further details about the affiliation of each node are reported in Table S1. The predictive models will be made publicly available at https://github.com/emergelab.

connectivity in the rostral anterior cingulate cortex (ACC; Figure 1A). However, the latter finding lost significance in the predictive model analysis (Figure 1B). Intriguingly, although GBC is a whole-brain based measure and not network restricted, the positive predictive GBC nodes were primarily located within the CE and GPu SC modules. Similarly, the negative predictive GBC nodes were primarily within the SM and VI networks (see Figures 1B vs. 3C). Although the primary analysis failed to show increased GBC in the lateral PFC as predicted by hypothesis 1, this may be due to limitations of the used vertex-/voxel-wise approach (see below) Supplemental Information.

The interpretive NRS model confirmed the predictions of hypothesis 2, showing significant association between better response to sertraline at week 8 and earlier reduction in internal DM connectivity at week 1 post treatment. Follow-up analyses revealed increased CE-SM connectivity as early predictor of enhanced response to sertraline (Figure 2B).

Compared with placebo, the NRS-PMs significantly predicted response to sertraline, supporting hypothesis 3, while revealing dynamic shifts in the brain circuits, critically underlying the negative and positive predictions of treatment effects (Figures 4 and 5). In particular, three patterns of connectivity shifts have emerged as predictors of response to antidepressant treatment: (1) A reduction in internal connectivity among the CE and GPu SC modules, along with increased external connectivity between these modules and the rest of the brain (most evident in AA-50, but also in AA-24, and niNRS/neNRS). (2) Reduced internal connectivity among modules within the SM and VI networks. (3) In DM/VS modules containing the

amygdala and insula (i.e., affective DM and inferior VS, respectively), there was reduced connectivity with perceptual and motor areas (i.e., SM and VI) but increased connectivity with higher order association regions, suggesting an early shift toward enhanced executive control Supplemental Information.

The current study focused on the changes overtime in brain functional connectivity and in psychopathology as reflected by antidepressant scores. This focused approach provided a powerful comprehensive assessment of brain connectivity in relation to treatment response. However, future complementary and follow-up studies are still required to determine whether pretreatment connectivity, as well as clinical features (e.g., early life stress or symptom clusters) would be associated with specific CFPs or would predict response to antidepressants. Notably, an outstanding recent study has investigated pretreatment connectivity and clinical features in the EMBARC cohort (Yu et al., 2019). Before treatment, it was reported that various brain networks correlated with early life stressors and that MDD was characterized by increased NRS in intrinsic networks, including DM, but reduced NRS in task-positive networks, including CE (Yu et al., 2019). Importantly, these pretreatment findings of altered DM and CE connectivity in MDD suggest that the antidepressant CFP identified in the current study may reflect an early pattern of normalization detectable biologically at week 1 but not evident behaviorally until week 8.

In the context of inconsistent patterns in the literature, we did not *a priori* predict the widespread role of the CE network at multiple hierarchical architectures, even though previous results from our own studies have associated increased GBC in the lateral PFC and caudate with enhanced antidepressant response (Abdallah et al., 2017b, 2018a). Better understanding of this oversight may be essential to enhance reproducibility in psychiatric neuroimaging studies. We believe that this oversight was primarily due to two common limitations of neuroimaging work. The first is that vertex-/voxel-wise traditional statistics (i.e., interpretive models, e.g., regression) are subject to overfitting owing to the lack of cross-validation and to type II error owing to the needed correction for multiple comparison. For example, an increase in vertex-wise GBC in the rostral ACC was identified in the interpretive analysis (Figure 1A) but did not hold when subjected to cross-validation procedures (Figure 1B). Moreover, the vertex-/voxel-wise interpretive model identifies only the peak effect (i.e., the vertices/voxels with the highest effect size), without the ability to fully map the behavioral brain effects (see Figures 1A vs. 1B). The second limitation is that the majority of ICN atlases were not multiscale hierarchical (i.e., lacking the information about the upstream ICN architecture) and were limited to the cortex (e.g., Yeo et al., 2011). The few ICN atlases that included subcortical structures were mostly post hoc (i.e., projecting the cortical ICNs on the subcortical regions without the use of a unified definition of ICN community; e.g., Choi et al., 2012) or were meta-analytically based missing important subcortical structures (e.g., the amygdala in Power et al., 2011). Thus, it was not commonly viewed that the caudate and frontoparietal cortex share the same upstream CE architecture. Furthermore, the biased focus of the literature on few key seeds and ICNs (e.g., DM) may have contributed to the apparent inconsistency across studies. In the current study, the full assessment of the connectome along with combined use of predictive models, hierarchical ICN architecture, and unified definition of ICN across cortical and subcortical nodes led to the robust identification of the CE ICN as critical predictor of treatment response using multiple data-driven analytical approaches.

In summary, based on the behavioral assessment of depression, there was no clinically meaningful behavioral response at week 1 (~2 points reduction on HAMD) and there were no significant differences between the treatment arms. In contrast, the biological functional connectivity investigation at week 1 showed a robust connectomic signature that predates and predicts response to sertraline at week 8. The identified biosignature was evident using three distinct, yet overlapping and complimentary, approaches. A main impact of the findings is the identification of an antidepressant-related dynamic shift in brain networks connectivity, which is consistent with early increase in executive control weeks prior to the full therapeutic behavioral effects. Some features of the identified connectomic signature are reminiscent of findings with ketamine, and the predictive models at least partially generalized to ketamine treatment, raising the possibility that the discovered connectome fingerprint may generalize to antidepressants with differing mechanism of action.

Future studies can capitalize on the established set of approaches that combine the strengths of consensus hierarchical architecture of the brain, along with neuroscience-informed features engineering and machine learning to fully assess the functional connectome and successfully identify psychopathology-relevant

reproducible fingerprint. These data-driven approaches are likely to have impact beyond answering the research question of the current study, by allowing the full assessment of functional connectivity in relation to behavior without the reliance on a limited number of seeds or networks. Together, the study findings enriched our understanding of the neurobiology of depression and revealed a previously unknown connectomic signature that may serve as a treatment target, as a biological indicator of response to optimize treatment regimen, or as a surrogate for early stages in drug development.

Limitation of the Study

The relatively small sample in the ketamine study is considered a limitation. Thus, the generalizability finding of the identified monoaminergic CFP to glutamatergic rapid acting antidepressants should be considered pilot evidence. In particular, using an active control, we found that ketamine induced a CFP highly comparable with the one identified with sertraline, which predated and predicted the rapid acting antidepressant effects (Figures 4 and 6). However, this was not the case when normal saline was used as control. It is plausible that the direct NMDA antagonism effects on pyramidal neurons are not fully required for the antidepressant properties of ketamine; thus, removing these non-specific effects using an active comparator may have facilitated the identification of the unique connectivity signature. This hypothesis would be consistent with accumulating evidence underscoring the role of the ketamine metabolite, (2R-6R)-hydroxynorketamine, which does not exert direct NMDA antagonistic effects (Riggs et al., 2019; Zanos et al., 2016, 2019). Yet, it remains important to highlight the pilot nature of this follow-up analysis and the need for replication in a larger sample prior to making any firm conclusions.

METHODS

All methods can be found in the accompanying Transparent Methods supplemental file.

DATA AND CODE AVAILABILITY

The study data are available through the Human Connectome Project (https://www.humanconnectome.org) and the National Institute of Mental Health (NIMH) Data Archive (NDA; https://nda.nih.gov/). The developed Akiki-Abdallah hierarchical modularity atlas, the network-restricted strength function, and the predictive model codes will be made publicly available at https://github.com/emergelab along with the predictive models established in the current paper.

SUPPLEMENTAL INFORMATION

Supplemental Information can be found online at https://doi.org/10.1016/j.isci.2019.100800.

ACKNOWLEDGMENTS

The authors would like to thank the subjects who participated in these studies for their invaluable contribution. Data used in the preparation of this manuscript were obtained and analyzed from the controlled access datasets distributed from the NIMH-supported National Database for Clinical Trials (NDCT). NDCT is a collaborative informatics system created by the National Institute of Mental Health to provide a national resource to support and accelerate discovery related to clinical trial research in mental health. Dataset identifier(s): STU 092010-151; Establishing Moderators and Biosignatures of Antidepressant Response for Clinical Care (EMBARC). Data were provided in part by the Human Connectome Project, WU-Minn Consortium (Principal Investigators: David Van Essen and Kamil Ugurbil; 1U54MH091657) funded by the 16 NIH Institutes and Centers that support the NIH Blueprint for Neuroscience Research; and by the McDonnell Center for Systems Neuroscience at Washington University. This manuscript reflects the views of the authors and may not reflect the opinions or views of the NIMH or of the Submitters submitting original data to NDCT.

Funding support was provided by NIMH (K23MH101498), VA Career Development Award (L.A.A.), the VA National Center for PTSD, and AstraZeneca. We are grateful for the expert assistance of the staff of the Clinical Research Facilities in Manchester and Oxford in which the ketamine study was conducted. P1vital managed the original ketamine study on behalf of AstraZeneca. The content of this report is solely the responsibility of the authors and does not necessarily represent the official views of the sponsors, the Department of Veterans Affairs, NIH, or the US Government.

AUTHOR CONTRIBUTIONS

Conceptualization, C.G.A., T.J.A., and S.N.; Methodology, C.G.A. and T.J.A.; Formal Analysis, C.G.A., T.J.A., and S.N.; Investigation, S.N., T.J.A., J.R., C.L.A., S.F., A.D., S.M., J.F.W.D., and C.G.A.; Writing – Original Draft, C.G.A., T.J.A., S.N., Y.J., and C.L.A.; Writing – Review/Editing, all authors; Funding Acquisition, C.G.A., L.A.A., J.H.K., and J.F.W.D.; Resources, C.G.A. and L.A.A.; Supervision, C.G.A., L.A.A., J.H.K., and J.F.W.D.

DECLARATION OF INTERESTS

Dr. Abdallah has served as a consultant and speaker and/or on advisory boards for Genentech, Janssen, Lundbeck, and FSV7 and editor of *Chronic Stress* for Sage Publications, Inc. and filed a patent for using mTORC1 inhibitors to augment the effects of antidepressants (filed on Aug 20, 2018). Dr. Krystal is a consultant for AbbVie, Inc., Amgen, Astellas Pharma Global Development, Inc., AstraZeneca Pharmaceuticals, Biomedisyn Corporation, Bristol-Myers Squibb, Eli Lilly and Company, Euthymics Bioscience, Inc., Neurovance, Inc., FORUM Pharmaceuticals, Janssen Research & Development, Lundbeck Research USA, Novartis Pharma AG, Otsuka America Pharmaceutical, Inc., Sage Therapeutics, Inc., Sunovion Pharmaceuticals, Inc., and Takeda Industries; is on the Scientific Advisory Board for Lohocla Research Corporation, Mnemosyne Pharmaceuticals, Inc., Naurex, Inc., and Pfizer; is a stockholder in Biohaven Pharmaceuticals; holds stock options in Mnemosyne Pharmaceuticals, Inc.; holds patents for Dopamine and Noradrenergic Reuptake Inhibitors in Treatment of Schizophrenia, U.S. Patent No. 5,447,948 (issued Sep 5, 1995), and Glutamate Modulating Agents in the Treatment of Mental Disorders, U.S. Patent No. 8,778,979 (issued Jul 15, 2014); and filed a patent for Intranasal Administration of Ketamine to Treat Depression – U.S. Application No. 14/197,767 (filed on Mar 5, 2014); U.S. application or Patent Cooperation Treaty international application No. 14/306,382 (filed on Jun 17, 2014). Filed a patent for using mTORC1 inhibitors to augment the effects of antidepressants (filed on Aug 20, 2018). Dr. Deakin currently advises or carries out research funded by Autifony, Sunovion, Lundbeck, AstraZeneca, and Servier. All other co-authors declare no conflict of interest.

Received: September 11, 2019
Revised: November 20, 2019
Accepted: December 18, 2019
Published: January 24, 2020

REFERENCES

Abdallah, C.G., Averill, C.L., Salas, R., Averill, L.A., Baldwin, P.R., Krystal, J.H., Mathew, S.J., and Mathalon, D.H. (2017a). Prefrontal connectivity and glutamate transmission: relevance to depression pathophysiology and ketamine treatment. Biol. Psychiatry Cogn. Neurosci. Neuroimaging *2*, 566–574.

Abdallah, C.G., Averill, L.A., Collins, K.A., Geha, P., Schwartz, J., Averill, C., DeWilde, K.E., Wong, E., Anticevic, A., Tang, C.Y., et al. (2017b). Ketamine treatment and global brain connectivity in major depression. Neuropsychopharmacology *42*, 1210–1219.

Abdallah, C.G., Dutta, A., Averill, C.L., McKie, S., Akiki, T.J., Averill, L.A., and William Deakin, J. (2018a). Ketamine, but not the NMDAR antagonist lanicemine, increases prefrontal global connectivity in depressed patients. Chronic Stress (Thousand Oaks) *2*, 2470547018796102.

Abdallah, C.G., Sanacora, G., Duman, R.S., and Krystal, J.H. (2018b). The neurobiology of depression, ketamine and rapid-acting antidepressants: is it glutamate inhibition or activation? Pharmacol. Ther. *190*, 148–158.

Akiki, T.J., and Abdallah, C.G. (2019). Determining the hierarchical architecture of the human brain using subject-level clustering of functional networks. Sci. Rep. *9*, 19290.

Akiki, T.J., Averill, C.L., Wrocklage, K.M., Scott, J.C., Averill, L.A., Schweinsburg, B., Alexander-Bloch, A., Martini, B., Southwick, S.M., Krystal, J.H., and Abdallah, C.G. (2018). Default mode network abnormalities in posttraumatic stress disorder: a novel network-restricted topology approach. Neuroimage *176*, 489–498.

Alexopoulos, G.S., Hoptman, M.J., Kanellopoulos, D., Murphy, C.F., Lim, K.O., and Gunning, F.M. (2012). Functional connectivity in the cognitive control network and the default mode network in late-life depression. J. Affect. Disord. *139*, 56–65.

Andrews, G. (2001). Placebo response in depression: bane of research, boon to therapy. Br. J. Psychiatry *178*, 192–194.

Andrews-Hanna, J.R., Smallwood, J., and Spreng, R.N. (2014). The default network and self-generated thought: component processes, dynamic control, and clinical relevance. Ann. N Y Acad. Sci. *1316*, 29–52.

Ban, T.A. (2006). The role of serendipity in drug discovery. Dialogues Clin. Neurosci. *8*, 335–344.

Bullmore, E., and Sporns, O. (2009). Complex brain networks: graph theoretical analysis of structural and functional systems. Nat. Rev. Neurosci. *10*, 186–198.

Choi, E.Y., Yeo, B.T., and Buckner, R.L. (2012). The organization of the human striatum estimated by intrinsic functional connectivity. J. Neurophysiol. *108*, 2242–2263.

Cole, M.W., Anticevic, A., Repovs, G., and Barch, D. (2011). Variable global dysconnectivity and individual differences in schizophrenia. Biol. Psychiatry *70*, 43–50.

Coplan, J.D., Gopinath, S., Abdallah, C.G., and Berry, B.R. (2014). A neurobiological hypothesis of treatment-resistant depression - mechanisms for selective serotonin reuptake inhibitor non-efficacy. Front. Behav. Neurosci. *8*, 189.

Downey, D., Dutta, A., McKie, S., Dawson, G.R., Dourish, C.T., Craig, K., Smith, M.A., McCarthy, D.J., Harmer, C.J., Goodwin, G.M., et al. (2016). Comparing the actions of lanicemine and ketamine in depression: key role of the anterior cingulate. Eur. Neuropsychopharmacol. *26*, 994–1003.

Etkin, A., Maron-Katz, A., Wu, W., Fonzo, G.A., Huemer, J., Vertes, P.E., Patenaude, B., Richiardi,

J., Goodkind, M.S., Keller, C.J., et al. (2019). Using fMRI connectivity to define a treatment-resistant form of post-traumatic stress disorder. Sci. Transl. Med. *11*, eaal3236.

Finn, E.S., Shen, X., Scheinost, D., Rosenberg, M.D., Huang, J., Chun, M.M., Papademetris, X., and Constable, R.T. (2015). Functional connectome fingerprinting: identifying individuals using patterns of brain connectivity. Nat. Neurosci. *18*, 1664–1671.

Galatzer-Levy, I.R., Ruggles, K., and Chen, Z. (2018). Data science in the research domain criteria era: relevance of machine learning to the study of stress pathology, recovery, and resilience. Chronic Stress *2*, https://doi.org/10.1177/2470547017747553.

Greicius, M.D., Flores, B.H., Menon, V., Glover, G.H., Solvason, H.B., Kenna, H., Reiss, A.L., and Schatzberg, A.F. (2007). Resting-state functional connectivity in major depression: abnormally increased contributions from subgenual cingulate cortex and thalamus. Biol. Psychiatry *62*, 429–437.

Gu, S., Satterthwaite, T.D., Medaglia, J.D., Yang, M., Gur, R.E., Gur, R.C., and Bassett, D.S. (2015). Emergence of system roles in normative neurodevelopment. Proc. Natl. Acad. Sci. U S A *112*, 13681–13686.

Guimera, R., and Amaral, L.A. (2005). Cartography of complex networks: modules and universal roles. J. Stat. Mech. *2005*, nihpa35573.

Holmes, S.E., Scheinost, D., Finnema, S.J., Naganawa, M., Davis, M.T., DellaGioia, N., Nabulsi, N., Matuskey, D., Angarita, G.A., Pietrzak, R.H., et al. (2019). Lower synaptic density is associated with depression severity and network alterations. Nat. Commun. *10*, 1529.

Kaiser, R.H., Andrews-Hanna, J.R., Wager, T.D., and Pizzagalli, D.A. (2015). Large-scale network dysfunction in major depressive disorder: a meta-analysis of resting-state functional connectivity. JAMA psychiatry *72*, 603–611.

Mulders, P.C., van Eijndhoven, P.F., Schene, A.H., Beckmann, C.F., and Tendolkar, I. (2015). Resting-state functional connectivity in major depressive disorder: a review. Neurosci. Biobehav. Rev. *56*, 330–344.

Murrough, J.W., Abdallah, C.G., Anticevic, A., Collins, K.A., Geha, P., Averill, L.A., Schwartz, J., DeWilde, K.E., Averill, C., Jia-Wei Yang, G., et al. (2016). Reduced global functional connectivity of the medial prefrontal cortex in major depressive disorder. Hum. Brain Mapp. *37*, 3214–3223.

Nusslock, R., Brody, G.H., Armstrong, C.C., Carroll, A.L., Sweet, L.H., Yu, T., Barton, A.W., Hallowell, E.S., Chen, E., Higgins, J.P., et al. (2019). Higher peripheral inflammatory signaling associated with lower resting-state functional brain connectivity in emotion regulation and central executive networks. Biol. Psychiatry *86*, 153–162.

Pizzagalli, D.A., Webb, C.A., Dillon, D.G., Tenke, C.E., Kayser, J., Goer, F., Fava, M., McGrath, P., Weissman, M., Parsey, R., et al. (2018). Pretreatment rostral anterior cingulate cortex Theta activity in relation to symptom improvement in depression: a randomized clinical trial. JAMA psychiatry *75*, 547–554.

Power, J.D., Cohen, A.L., Nelson, S.M., Wig, G.S., Barnes, K.A., Church, J.A., Vogel, A.C., Laumann, T.O., Miezin, F.M., Schlaggar, B.L., and Petersen, S.E. (2011). Functional network organization of the human brain. Neuron *72*, 665–678.

Riggs, L.M., Aracava, Y., Zanos, P., Fischell, J., Albuquerque, E.X., Pereira, E.F.R., Thompson, S.M., and Gould, T.D. (2019). (2R,6R)-hydroxynorketamine rapidly potentiates hippocampal glutamatergic transmission through a synapse-specific presynaptic mechanism. Neuropsychopharmacology *45*, 426–436.

Scheinost, D., Holmes, S.E., DellaGioia, N., Schleifer, C., Matuskey, D., Abdallah, C.G., Hampson, M., Krystal, J.H., Anticevic, A., and Esterlis, I. (2018). Multimodal investigation of network level effects using intrinsic functional connectivity, anatomical covariance, and structure-to-function correlations in unmedicated major depressive disorder. Neuropsychopharmacology *43*, 1119–1127.

Scheinost, D., Noble, S., Horien, C., Greene, A.S., Lake, E.M., Salehi, M., Gao, S., Shen, X., O'Connor, D., Barron, D.S., et al. (2019). Ten simple rules for predictive modeling of individual differences in neuroimaging. Neuroimage *193*, 35–45.

Schultz, D.H., Ito, T., Solomyak, L.I., Chen, R.H., Mill, R.D., Anticevic, A., and Cole, M.W. (2018). Global connectivity of the fronto-parietal cognitive control network is related to depression symptoms in the general population. Netw. Neurosci. *3*, 107–123.

Sexton, C.E., Allan, C.L., Le Masurier, M., McDermott, L.M., Kalu, U.G., Herrmann, L.L., Maurer, M., Bradley, K.M., Mackay, C.E., and Ebmeier, K.P. (2012). Magnetic resonance imaging in late-life depression: multimodal examination of network disruption. Arch. Gen. Psychiatry *69*, 680–689.

Sheline, Y.I., Price, J.L., Yan, Z., and Mintun, M.A. (2010). Resting-state functional MRI in depression unmasks increased connectivity between networks via the dorsal nexus. Proc. Natl. Acad. Sci. U S A *107*, 11020–11025.

Shen, X., Finn, E.S., Scheinost, D., Rosenberg, M.D., Chun, M.M., Papademetris, X., and Constable, R.T. (2017). Using connectome-based predictive modeling to predict individual behavior from brain connectivity. Nat. Protoc. *12*, 506–518.

Trivedi, M.H., Fava, M., Wisniewski, S.R., Thase, M.E., Quitkin, F., Warden, D., Ritz, L., Nierenberg, A.A., Lebowitz, B.D., Biggs, M.M., et al. (2006). Medication augmentation after the failure of SSRIs for depression. N. Engl. J. Med. *354*, 1243–1252.

Trivedi, M.H., McGrath, P.J., Fava, M., Parsey, R.V., Kurian, B.T., Phillips, M.L., Oquendo, M.A., Bruder, G., Pizzagalli, D., Toups, M., et al. (2016). Establishing moderators and biosignatures of antidepressant response in clinical care (EMBARC): Rationale and design. J. Psychiatr. Res. *78*, 11–23.

Van Essen, D.C., Smith, S.M., Barch, D.M., Behrens, T.E., Yacoub, E., and Ugurbil, K.; WU-Minn HCP Consortium (2013). The WU-Minn human connectome Project: an overview. Neuroimage *80*, 62–79.

Wang, L., Dai, Z., Peng, H., Tan, L., Ding, Y., He, Z., Zhang, Y., Xia, M., Li, Z., Li, W., et al. (2014). Overlapping and segregated resting-state functional connectivity in patients with major depressive disorder with and without childhood neglect. Hum. Brain Mapp. *35*, 1154–1166.

Wu, M., Andreescu, C., Butters, M.A., Tamburo, R., Reynolds, C.F., 3rd, and Aizenstein, H. (2011). Default-mode network connectivity and white matter burden in late-life depression. Psychiatry Res. *194*, 39–46.

Yang, Z., Gu, S., Honnorat, N., Linn, K.A., Shinohara, R.T., Aselcioglu, I., Bruce, S., Oathes, D.J., Davatzikos, C., Satterthwaite, T.D., et al. (2018). Network changes associated with transdiagnostic depressive symptom improvement following cognitive behavioral therapy in MDD and PTSD. Mol. Psychiatry *23*, 2314–2323.

Yeo, B.T., Krienen, F.M., Sepulcre, J., Sabuncu, M.R., Lashkari, D., Hollinshead, M., Roffman, J.L., Smoller, J.W., Zollei, L., Polimeni, J.R., et al. (2011). The organization of the human cerebral cortex estimated by intrinsic functional connectivity. J. Neurophysiol. *106*, 1125–1165.

Yu, M., Linn, K.A., Shinohara, R.T., Oathes, D.J., Cook, P.A., Duprat, R., Moore, T.M., Oquendo, M.A., Phillips, M.L., McInnis, M., et al. (2019). Childhood trauma history is linked to abnormal brain connectivity in major depression. Proc. Natl. Acad. Sci. U S A *116*, 8582–8590.

Zanos, P., Highland, J.N., Stewart, B.W., Georgiou, P., Jenne, C.E., Lovett, J., Morris, P.J., Thomas, C.J., Moaddel, R., Zarate, C.A., Jr., and Gould, T.D. (2019). (2R,6R)-hydroxynorketamine exerts mGlu2 receptor-dependent antidepressant actions. Proc. Natl. Acad. Sci. U S A *116*, 6441–6450.

Zanos, P., Moaddel, R., Morris, P.J., Georgiou, P., Fischell, J., Elmer, G.I., Alkondon, M., Yuan, P., Pribut, H.J., Singh, N.S., et al. (2016). NMDAR inhibition-independent antidepressant actions of ketamine metabolites. Nature *533*, 481–486.

iScience, Volume *23*

Supplemental Information

A Unique Brain Connectome Fingerprint Predates and Predicts Response to Antidepressants

Samaneh Nemati, Teddy J. Akiki, Jeremy Roscoe, Yumeng Ju, Christopher L. Averill, Samar Fouda, Arpan Dutta, Shane McKie, John H. Krystal, J.F. William Deakin, Lynnette A. Averill, and Chadi G. Abdallah

SUPPLEMENTAL INFORMATION

Transparent Methods

The data used in this study were collected as part of the Establishing Moderators and Biosignatures of Antidepressant Response in Clinical Care (EMBARC) trial (Trivedi et al., 2016), the Human Connectome Project (HCP) (Van Essen et al., 2013), and a previously published pharmacoimaging study (Abdallah et al., 2018; Downey et al., 2016). All studies were approved by Institutional Review Boards, and all participants signed informed consents.

Participants and Procedures of Sertraline Study

The current study included data from 202 individuals with MDD for whom the *f*MRI and behavioral assessments were available (Table 1). Participants were randomized to an 8-week course of up to 200 mg daily sertraline or to placebo. Depression severity was rated on the 17-item Hamilton Depression Rating Scale (HAMD) before and after treatment (Hamilton, 1967). The primary clinical outcome of the parent trial was treatment response which was defined as 50% reduction in HAMD score at week 8. Randomized participants were scanned and assessed at both baseline and week 1 of treatment. Then, they continued to take medication for a total of 8 weeks. Their HAMD scores were assessed again at the end of week 8.

Eligible participants between 18 and 65 years old, met criteria for nonpsychotic MDD as per the Structured Clinical Interview for DSM-IV-TR (SCID) criteria (First et al., 2002), had a Quick Inventory of Depressive Symptomatology (QIDS) (Rush et al., 2003) score equal or above 14, and were unmedicated for at least 3 weeks prior to the study (Trivedi et al., 2016).

Participants and Procedures of Ketamine Study

The current study included data from 56 individuals with MDD for whom the *f*MRI and behavioral assessments were available. Participants were randomized to a single intravenous infusion of normal saline (inactive control; n = 18), lanicemine (100mg; active control; n = 19), or ketamine (0.5mg/kg; n = 19). Depression severity was rated on the Beck Depression Inventory (BDI) before and at 24h after treatment (Beck, 1996). Randomized participants were scanned and assessed at both baseline and during infusion of the study drugs. Further details can be found at the following references (Abdallah et al., 2018; Downey et al., 2016).

Neuroimaging Acquisition and Processing

Sertraline study structural (1x1x1 mm^3) and functional (3.2x3.2x3.1 mm^3; TR=2000 ms.; TE=28 ms.; 12 min. at baseline and week 1) scans, and ketamine study structural (1x1x1 mm^3) and functional (3x3x2.5 mm^3; TR=3000 ms.; TE=30 ms.; 5min. immediately prior to infusion and 20 min. during infusion starting at 20 min post administration) scans were acquired using 3.0 T magnets (Abdallah et al., 2018; Downey et al., 2016; Greenberg et al., 2015). Brain scans from both studies underwent the same surface-based preprocessing using pipeline adapted from the HCP (https://github.com/Washington-University/HCPpipelines) (Glasser et al., 2013), as reported elsewhere (Abdallah et al., 2019a; Abdallah et al., 2019b; Abdallah et al., 2018). Briefly, the preprocessing pipeline included FreeSurfer parcellation of structural scans, slice timing correction, motion correction, intensity normalization, brain masking, and registration of *f*MRI images to structural MRI and standard template. Then, the cortical gray matter ribbon voxels and each subcortical parcel were projected to a standard Connectivity Informatics Technology Initiative (CIFTI) 2mm grayordinate space. ICA-FIX was run to identify and remove artifacts (Griffanti et al., 2014; Salimi-Khorshidi et al., 2014), followed by mean grayordinate time series regression (MGTR). The latter two processing steps (FIX+MGTR) have been found to significantly reduce motion-correlated artifacts (Burgess et al., 2016). Global brain connectivity (GBC) was computed voxel/vertex-

wise (Abdallah et al., 2019b); i.e., the average correlation of each voxel/vertex with all other gray matter voxels and vertices (Cole et al., 2011).

Nodal Parcellation and Network Restriction

The brain nodes were defined using previously established multimodal parcellation atlases that divide the cerebral cortex (Glasser et al., 2016), subcortical regions (Fan et al., 2016), and the cerebellum (Diedrichsen et al., 2009) into 424 nodes within the grayordinate (Table S1), here termed A424. Within each node, an averaged time series of all voxels/vertices was calculated. The full connectome was computed as the pairwise Pearson correlation coefficients between these averaged time series, and subsequently transformed using a Fisher-z function. Nodal strength (nS) was computed as the average connectivity between each node and all other nodes within the full connectome.

To define the network modules, we used the Akiki-Abdallah cortical (AAc) atlas (Akiki and Abdallah, 2019), a recently described hierarchical modular organization of the cortex based on the same parcellation atlas used in the current study. The AAc atlas provided an extensive characterization of the cortical modules at multiple scales, ranging from three communities at the first hierarchical split to 126 communities at the finest-grained level.

To test the hypothesis that the connectivity in the canonical networks can predict treatment response, we used the AAc architecture at 6 modules (AAc-6), i.e., the level that fully map the default mode (DM; i.e., the target network for hypothesis #2), and which also comprises modules for the central executive (CE), dorsal salience (DS), ventral salience (VS), somatomotor (SM), and visual (VI) networks (Akiki and Abdallah, 2019). For each network (a.k.a., module or community), the internal network-restricted strength (NRS) was calculated as the mean weight of edges within a given network (Akiki et al., 2018a, b). The external pairwise network-to-network (e.g., DM-to-CE) NRS was also calculated as the mean edge weight between the two respective networks.

Since the modular organization (a.k.a., intrinsic connectivity networks; ICNs) is primarily defined in the cerebral cortex (Schaefer et al., 2018; Yeo et al., 2011), the initial NRS analyses were limited to the cortical surface (i.e., 360 nodes (Glasser et al., 2016)). However, considering the essential role of non-cortical brain structures in pathophysiology of depression (Drevets, 1998), and that the GBC findings spanned several subcortical structures, we pursued complementary NRS analyses including the whole-brain grayordinate (i.e., A424 atlas (Diedrichsen et al., 2009; Fan et al., 2016; Glasser et al., 2016)). Using the methods implemented in the AAc atlas (Akiki and Abdallah, 2019), we first determined the hierarchical architecture of the whole-brain using subject-level clustering of functional networks in 1003 healthy subjects from the HCP, here termed Akiki-Abdallah (AA) atlas. For full details of the scans preprocessing and modularity methods, please see (Akiki and Abdallah, 2019). Briefly, the processing included the preprocessed HCP data with FIX+MGTR (Glasser et al., 2013) and the modularity methods used a subject-level clustering approach followed by a recursive hierarchical method based on the Louvain algorithm to recover the community structure at multiple scales (Jeub et al., 2018; Jutla et al., 2011; MacMahon and Garlaschelli, 2013; Subelj and Bajec, 2011). A critical aspect is that all brain nodes were considered together, rather than projecting the cortical ICNs onto subcortical nodes. As previously implemented (Akiki and Abdallah, 2019), we used the z-score of the Rand coefficient to identify partition solutions in the consensus hierarchy that are highly expressed at the level of individual subjects (Bassett et al., 2013; Betzel et al., 2015; Doron et al., 2012; Traud et al., 2011).

Predictive Modeling

Traditional interpretative analyses are informative in that they can highlight links between brain and behavior. However, they may not be adequate to predict outcomes and could suffer from over-fitting (Scheinost et al., 2019). The connectome predictive model (CPM) described by Shen et al. (Shen et al., 2017), takes full connectome matrices as inputs and its utility has been well validated in multiple studies (e.g., (Finn et al., 2015)). Building on the strengths of CPM, we here implemented 4 comparable approaches, 1) termed nodal strength

predictive model (nS PM); 2) termed NRS predictive model (NRS-PM) – Please see "hypothesis 2" and "hypothesis 3" in the supplemental information (SI) for rationale and justification; 3) termed nodal external NRS-PM (neNRS-PM), and 4) termed nodal internal NRS-PM (niNRS-PM).

The NRS-PM builds a predictive model of the behavioral data based on NRS edges (i.e., internal and external connectivity). The first step serves as feature selection: the within- and between-network connectivity values (i.e., edges) from the training subset of the data (described below) are used in regression models (Pearson correlation) to identify NRS edges that positively or negatively predict the behavioral measure of interest ($p < 0.05$). The weighted sum of positive edges minus the weighted sum of negative edges generate a summary statistic for each subject that is then included in a linear predictive model (Shen et al., 2017). Next, as described by Shen et al. (Shen et al., 2017), the resulting coefficients are applied to the test dataset to predict the outcome. The correlations between the predicted and actual outcomes (*r* values) were used to judge the model's performance (Shen et al., 2017). To ensure the stability of the models and to determine the significance of the predictive power, we used 1000 iterations of ten-fold cross-validation (CV), which splits the original sample into 10 random equal sized subsamples. In each iteration, one subsample (10% of subjects) is retained as the validation data for testing the model, and the remaining 9 subsamples (90% of subjects) are used as training data. The cross-validation process is then repeated 10 times (covering all subsamples). Then, the predicted outcome was separately correlated with the true outcome (i.e., true prediction) and with a random permutation of the true outcome (i.e., random prediction). This process was repeated 1000 times to generate empirical true and null distributions of the test statistics (i.e., *r*). The *p* values were then computed as the proportion of random predictions that are equal to or greater than the average of true predictions.

The a priori hierarchical level was the AAc brain architecture with 22 modules (AAc-22), based on evidence that this organization is the most expressed at the level of individuals (Akiki and Abdallah, 2019). At this relatively fine-grained modular organization (Table S1), there are five visual communities (medial, inferolateral, para, midlateral, superolateral), four somatomotor communities (central, paracentral, inferior, auditory), three ventral salience communities (superior, posterior, inferior), two dorsal salience communities (superior, inferior), four central executive communities (right, left, limbic, dorsal anterior cingulate), and four default mode communities (medial, temporal, limbic, language). The AAc-22 NRS generates 22 within network edges (i.e., internal connectivity), and 231 unique module-to-module edges (i.e., upper triangle of pairwise external undirected connectivity; 22*21/2=231), for a total of 253 features. To assess the robustness of the findings, we applied the same analyses across all hierarchical levels.

The nS-PM, neNRS-PM, niNRS-PM, and full connectome PM (FC-PM) used the same approach described above for the NRS-PM, with the only difference is in the dimensionality reduction step. For nS-PM, the dimensionality reduction step was computing the average correlation between each node and all other nodes in the full connectome, which generates 424 features. For neNRS-PM, the dimensionality reduction step was computing the average correlation between each node and all other nodes outside its ICN, which generates 424 features. For niNRS-PM, the dimensionality reduction step was computing the average correlation between each node and all other nodes within the same ICN, which generates 424 features. For neNRS-PM and niNRS-PM, we first investigated the PMs at AA-7, then applied the same analyses to all hierarchical levels. For the FC-PM, the dimensionality reduction step was using the upper triangle of the full connectome, which includes 89676 (424*423/2) unique features.

Statistical analyses

The normality of outcome measures was checked and confirmed through normal probability plots and test statistics. The standard deviations of the sampling distribution of the mean were considered as estimates of variation. Chi-squares and t-tests were used to determine the difference in demographic data between the sertraline and placebo groups. For the GBC and interpretative NRS analyses, we used a general linear model to examine

the effect of treatment (sertraline vs. placebo), response (responder vs. non-responder), and their interaction on the connectivity changes from baseline to week one. Age, sex, and site were used as covariates. False Discovery Rate (FDR; $q < 0.05$) was used to correct for multiple comparisons. To assess the improvement-by-treatment interaction in the predictive models, the behavioral outcome was computed as the percent improvement in depression score (i.e., HAMD in the sertraline study and BDI in the ketamine study) multiplied by the treatment contrast (i.e., 1 for study drug and -1 for placebo control). The statistical significance threshold was set at 0.05 (2-tailed tests). MATLAB (2017b; Mathworks Inc.) and the Statistical Package for the Social Sciences (version 24; IBM) software were used for the analyses.

Cortical Network-Restricted Strength Predictive Model (NRS-PM)

Capitalizing on recent work determining the hierarchical ICNs architecture of the brain cortex (Akiki and Abdallah, 2019), we implemented a novel NRS-PM approach to establish a cortical connectomic signature that significantly predict improvement following sertraline compared to placebo. As the architecture with the highest similarity to subject-specific modularity (Akiki and Abdallah, 2019), the AAc-22 was selected for the initial analysis (Fig. S4). Changes in AAc-22 NRS at week-1 significantly predicted improvement at week-8 following sertraline compared to placebo ($r = 0.25$, $CV = 10$, $iterations = 1000$, $p = 0.005$). Increased external connectivity between modules within the CE and the rest of the cortex predicted better antidepressant response. Conversely, reduced internal connectivity between modules within the VI and SM ICNs predicted enhanced response to sertraline. Negative predictive edges were also found in DM-SM and VS-SM connections (Fig. S4).

Next, we examined whether the *a priori* selection of AAc-22 may have biased the results. Here, we conducted comparable NRS-PM across all cortical architectures (i.e., AAc-3 to AAc-126). We also examined whether the negative and positive predicators would independently predict the antidepressant response. As shown in Fig. S5A, the NRS-PM predicted the antidepressant response across all architectures, with a peak at AAc-21 ($r = 0.25$, $CV = 10$, $iterations = 1000$, $p = 0.003$). Independently, the positive predictive edges peaked at AAc-30 ($r = 0.21$, $CV = 10$, $iterations = 1000$, $p = 0.009$) and the negative predictive edges peaked at AAc-21 ($r = 0.25$, $CV = 10$, $iterations = 1000$, $p = 0.003$).

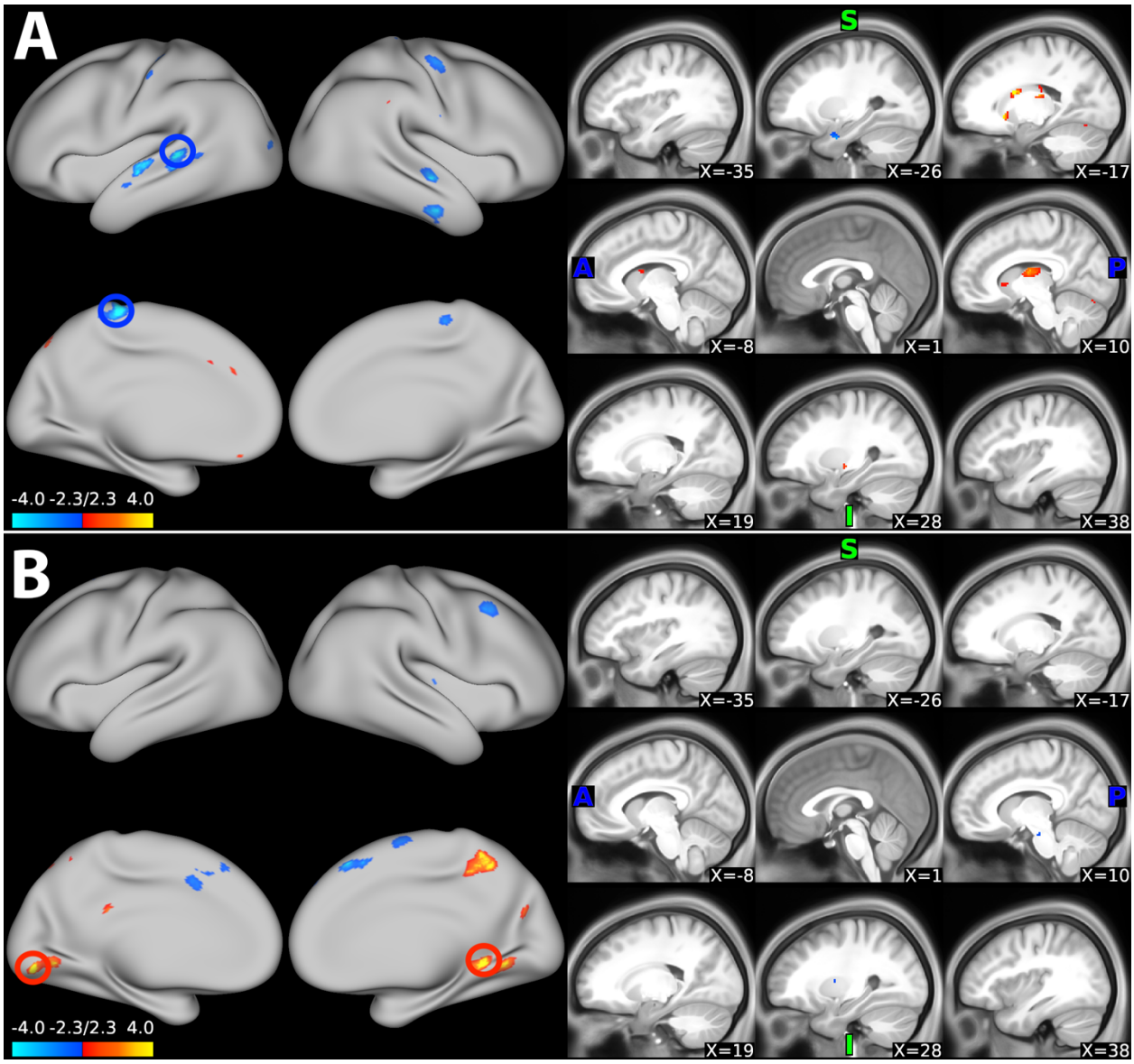

Figure S1. The Effect of Treatment and Response on Global Brain Connectivity (GBC). Related to Figure 1A. Cortical and subcortical results of the GBC analyses showing clusters that were different (A) in the sertraline vs. placebo groups and (B) in the responder vs. non-responder groups. The scale represents the *z* values (here showing voxels/vertices with $p < 0.005$, uncorrected). The circles represent clusters that survived FDR correction ($q < 0.05$).

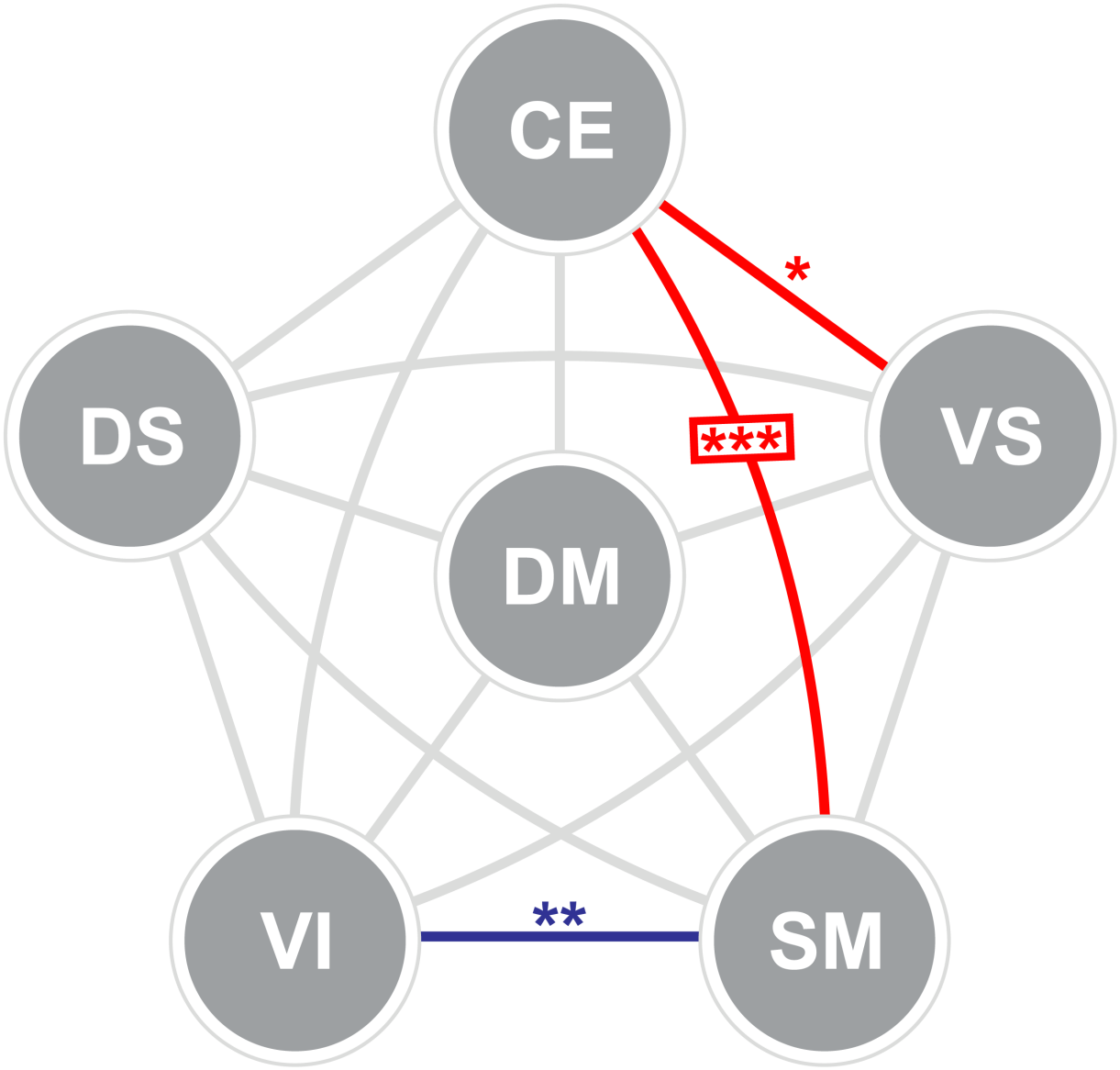

Figure S2. Interpretive Network-Restricted Strength (NRS) Analyses Showing the Effect of Treatment. Related to Figure 2. The network-restricted strength (NRS) pentagon. Internal NRS is depicted as filled circles, while inter-networks external NRS is depicted as edges. * was used for $p < 0.05$, ** for $p < 0.01$, *** for $p < 0.001$. Effects that survived FDR correction were denoted with squares (i.e., CE-SM edge). Filled circles and edges were colored gray for non-significant effects, blue for negative effects, and red for positive effects.

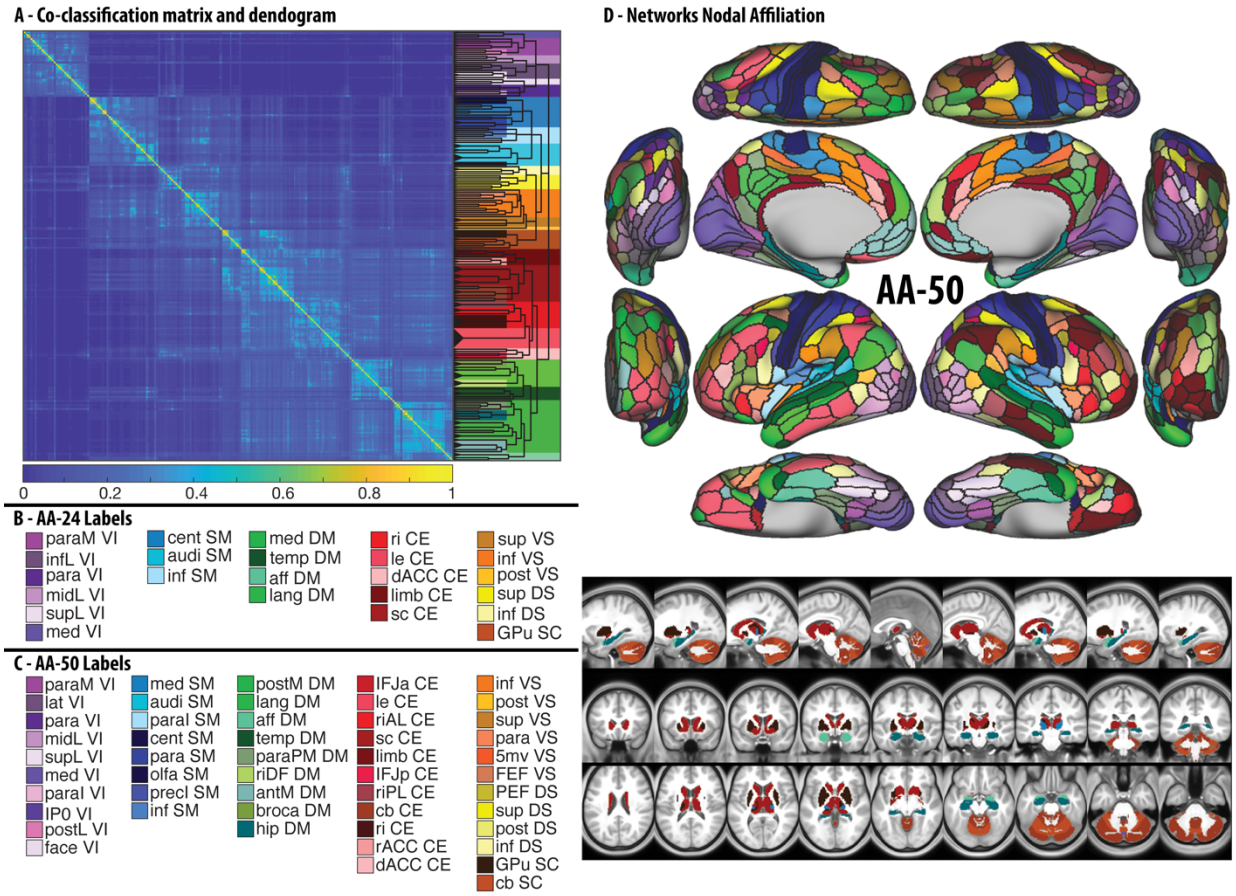

Figure S3. Co-classification Matrix and Dendrogram. Related to Figure 3. The dendrogram background colors (A) represent the whole-brain Akiki-Abdallah (AA) network affiliation at 24 modules architecture (i.e., AA-24; **B**) and at AA-50 (**C-D**). The module abbreviations of AA-24 and AA-50, along with further details about the affiliation of each node are reported in Table S1.

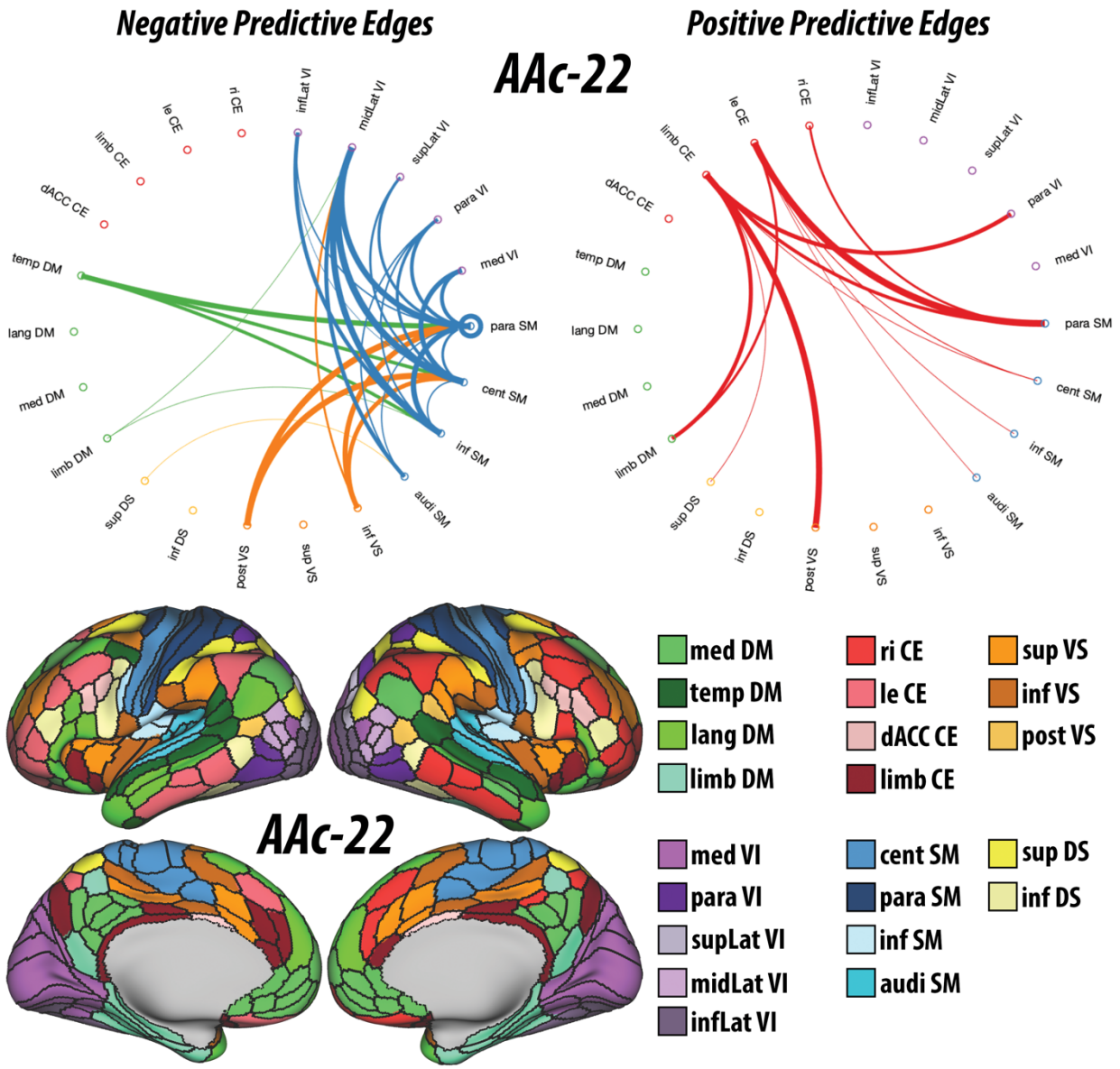

Figure S4. A Shift from Internal to External Connectivity Predicts Enhanced Antidepressant Response. Related to Figure 4. *Lower panel* shows the cortical networks nodal affiliation based on the Akiki-Abdallah hierarchical atlas at 22 modules (AAc-22; see Table S1 for abbreviations and further details) (Akiki and Abdallah, 2019). *The top panel* circular graphs depict the results of the cortical NRS predictive model (NRS-PM; $p = 0.005$). The modules are labeled based on the AAc-22 brain architecture. Modules are colored according to their AAc-6 network affiliation (Figure 2A). Edges are colored based on the initiating module using a counter-clockwise path starting at 12 o'clock. Internal edges (i.e., within module NRS; e.g., para SM to para SM edge) are depicted as outer circles around the corresponding module. Thickness of edges reflect their corresponding weight in the predictive model. The module abbreviations of AAc-22, along with further details about the affiliation of each node are reported in Table S1. Reduced internal connectivity among edges within SM and VI networks and increased connectivity between CE and the rest of the brain at week-1 predicted better response to sertraline at week-8, compared to placebo. Enhanced response to sertraline was also predicted by a shift from DM-SM and VS-SM to increased DM-CE and VS-CE. An overall pattern emerged, that is consistent with increased top down control and reduced affective interference with primary cortices. The NRS computation and predictive model codes will be made publicly available at https://github.com/emergelab.

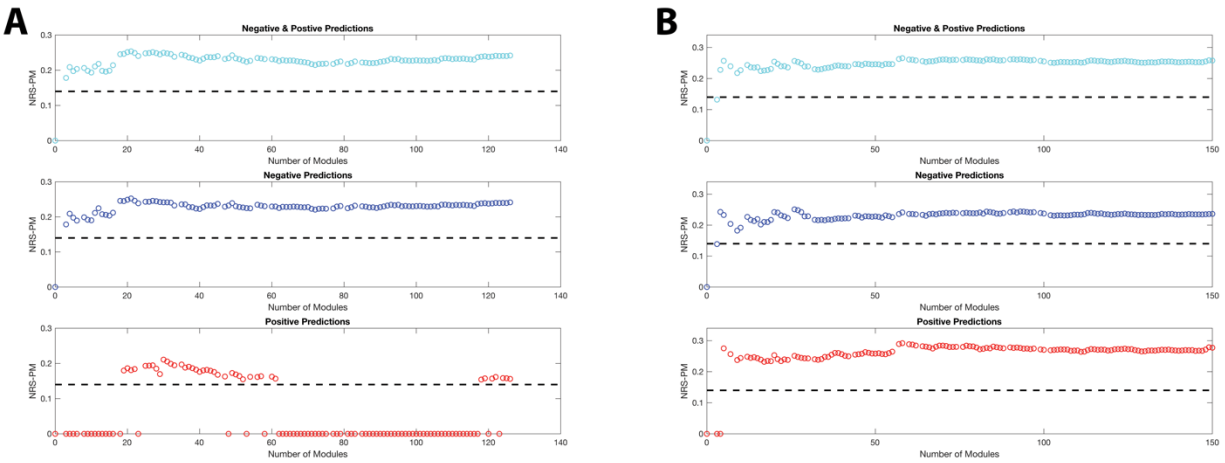

Figure S5. Robustness Analyses for the Network-Restricted Strength Predictive Models (NRS-PMs). Related to Figure 4. The performance of NRS-PM at all hierarchical levels using the cortical (**A**) and cortical/subcortical/cerebellar (**B**) modularity atlases. The vertical axes represent the performance of the models (quantified using *r* values) in predicting the response to sertraline and the horizontal axes represent the spatial scales (number of modules). The dashed line represents the *r* value corresponding to $p = 0.05$. Values set at 0 correspond to architectures that were not significant based on the permutation analysis.

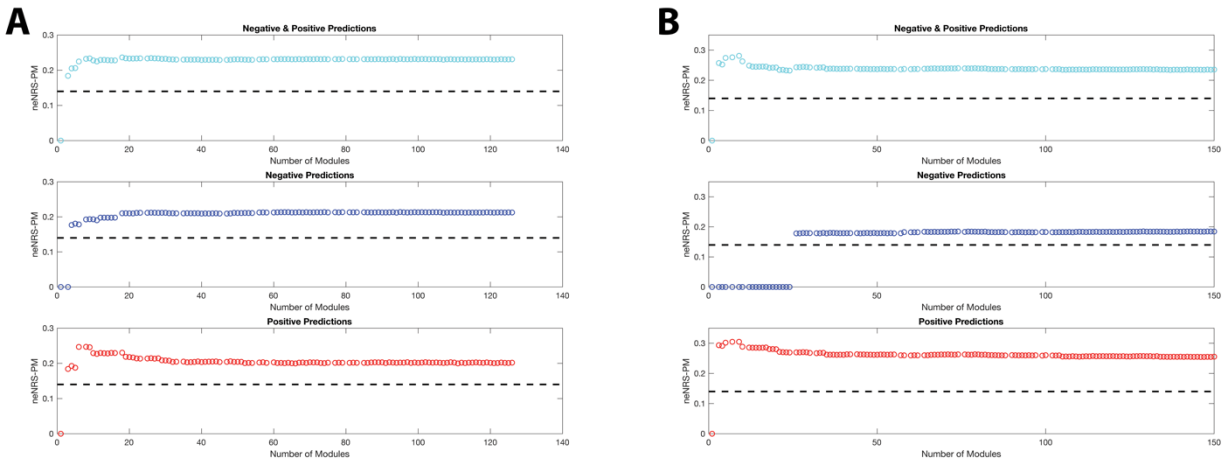

Figure S6. Robustness Analyses for the nodal external Network-Restricted Strength Predictive Models (neNRS-PMs). Related to Figure 5A-B. The performance of neNRS-PM at all hierarchical levels using the cortical (**A**) and cortical/subcortical (**B**) modularity atlases. The vertical axes represent the performance of the models (quantified using *r* values) in predicting the response to sertraline and the horizontal axes represent the spatial scales (number of modules). The dashed line represents the *r* value corresponding to $p = 0.05$. Values set at 0 correspond to architectures that were not significant based on the permutation analysis.

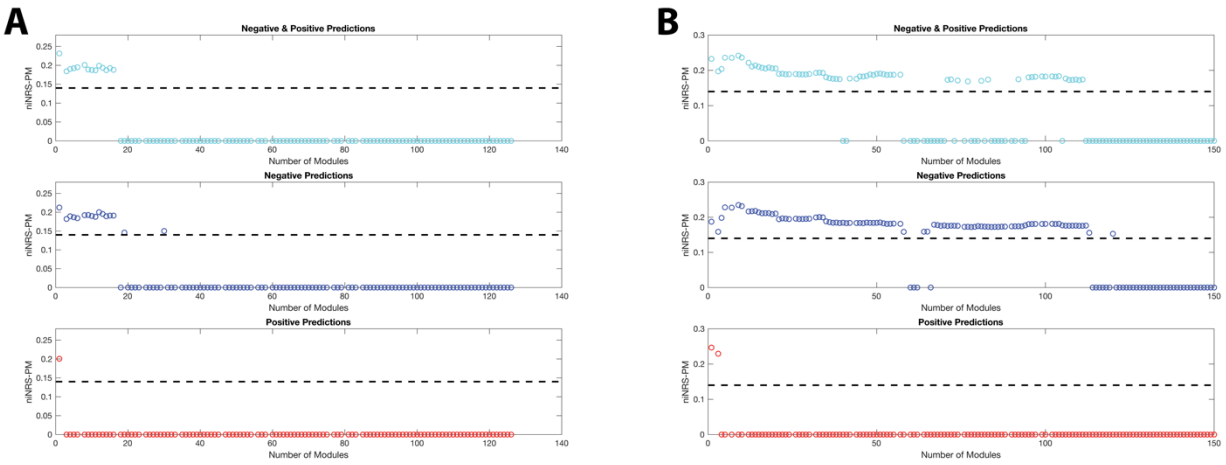

Figure S7. Robustness Analyses for the nodal internal Network-Restricted Strength Predictive Models (niNRS-PMs). Related to Figure 5C-D. The performance of niNRS-PM at all hierarchical levels using the cortical (**A**) and cortical/subcortical (**B**) modularity atlases. The vertical axes represent the performance of the models (quantified using *r* values) in predicting the response to sertraline and the horizontal axes represent the spatial scales (number of modules). The dashed line represents the *r* value corresponding to $p = 0.05$. Values set at 0 correspond to architectures that were not significant based on the permutation analysis.

Supplemental References

Abdallah, C.G., Averill, C.L., Ramage, A.E., Averill, L.A., Alkin, E., Nemati, S., Krystal, J.H., Roache, J.D., Resick, P., Young-McCaughan, S.*, et al.* (2019a). Reduced Salience and Enhanced Central Executive Connectivity Following PTSD Treatment. Chronic Stress 3, 2470547019838971.

Abdallah, C.G., Averill, C.L., Ramage, A.E., Averill, L.A., Goktas, S., Nemati, S., Krystal, J.H., Roache, J.D., Resick, P.A., Young-McCaughan, S.*, et al.* (2019b). Salience Network Disruption in U.S. Army Soldiers With Posttraumatic Stress Disorder. Chronic Stress 3, 2470547019850467.

Abdallah, C.G., Dutta, A., Averill, C.L., McKie, S., Akiki, T.J., Averill, L.A., and William Deakin, J. (2018). Ketamine, but Not the NMDAR Antagonist Lanicemine, Increases Prefrontal Global Connectivity in Depressed Patients. Chronic Stress 2, 2470547018796102.

Akiki, T.J., and Abdallah, C.G. (2019). Determining the Hierarchical Architecture of the Human Brain Using Subject-Level Clustering of Functional Networks. Scientific Reports 9, 19290.

Akiki, T.J., Averill, C.L., Wrocklage, K.M., Scott, J.C., Averill, L.A., Schweinsburg, B., Alexander-Bloch, A., Martini, B., Southwick, S.M., Krystal, J.H., and Abdallah, C.G. (2018a). Default mode network abnormalities in posttraumatic stress disorder: A novel network-restricted topology approach. Neuroimage 176, 489-498.

Akiki, T.J., Averill, C.L., Wrocklage, K.M., Scott, J.C., Averill, L.A., Schweinsburg, B., Alexander-Bloch, A., Martini, B., Southwick, S.M., Krystal, J.H., and Abdallah, C.G. (2018b). Topology of brain functional connectivity networks in posttraumatic stress disorder. Data in brief 20, 1658-1675.

Bassett, D.S., Porter, M.A., Wymbs, N.F., Grafton, S.T., Carlson, J.M., and Mucha, P.J. (2013). Robust detection of dynamic community structure in networks. Chaos 23, 013142.

Beck, A.T., Steer, R.A., Brown, G. (1996). Manual for the Beck Depression Inventory - II (San Antonio, Texas: Psychological Corporation).

Betzel, R.F., Mišić, B., He, Y., Rumschlag, J., Zuo, X.-N., and Sporns, O. (2015). Functional brain modules reconfigure at multiple scales across the human lifespan. arXiv preprint arXiv:151008045.

Burgess, G.C., Kandala, S., Nolan, D., Laumann, T.O., Power, J.D., Adeyemo, B., Harms, M.P., Petersen, S.E., and Barch, D.M. (2016). Evaluation of Denoising Strategies to Address Motion-Correlated Artifacts in Resting-State Functional Magnetic Resonance Imaging Data from the Human Connectome Project. Brain connectivity 6, 669-680.

Cole, M.W., Anticevic, A., Repovs, G., and Barch, D. (2011). Variable global dysconnectivity and individual differences in schizophrenia. Biol Psychiatry 70, 43-50.

Diedrichsen, J., Balsters, J.H., Flavell, J., Cussans, E., and Ramnani, N. (2009). A probabilistic MR atlas of the human cerebellum. Neuroimage 46, 39-46.

Doron, K.W., Bassett, D.S., and Gazzaniga, M.S. (2012). Dynamic network structure of interhemispheric coordination. Proc Natl Acad Sci U S A 109, 18661-18668.

Downey, D., Dutta, A., McKie, S., Dawson, G.R., Dourish, C.T., Craig, K., Smith, M.A., McCarthy, D.J., Harmer, C.J., Goodwin, G.M., *et al.* (2016). Comparing the actions of lanicemine and ketamine in depression: key role of the anterior cingulate. Eur Neuropsychopharmacol 26, 994-1003.

Drevets, W.C. (1998). Functional neuroimaging studies of depression: the anatomy of melancholia. Annu Rev Med 49, 341-361.

Fan, L., Li, H., Zhuo, J., Zhang, Y., Wang, J., Chen, L., Yang, Z., Chu, C., Xie, S., Laird, A.R., *et al.* (2016). The Human Brainnetome Atlas: A New Brain Atlas Based on Connectional Architecture. Cereb Cortex 26, 3508-3526.

Finn, E.S., Shen, X., Scheinost, D., Rosenberg, M.D., Huang, J., Chun, M.M., Papademetris, X., and Constable, R.T. (2015). Functional connectome fingerprinting: identifying individuals using patterns of brain connectivity. Nat Neurosci 18, 1664-1671.

First, M., Spitzer, R., Gibbon, M., and Williams, J. (2002). Structured clinical interview for DSM-IV-TR axis I disorders, research version, patient edition (SCID-I/P). (Biometrics Research, New York State Psychiatric Institute New York).

Glasser, M.F., Coalson, T.S., Robinson, E.C., Hacker, C.D., Harwell, J., Yacoub, E., Ugurbil, K., Andersson, J., Beckmann, C.F., Jenkinson, M., *et al.* (2016). A multi-modal parcellation of human cerebral cortex. Nature 536, 171-178.

Glasser, M.F., Sotiropoulos, S.N., Wilson, J.A., Coalson, T.S., Fischl, B., Andersson, J.L., Xu, J., Jbabdi, S., Webster, M., Polimeni, J.R., *et al.* (2013). The minimal preprocessing pipelines for the Human Connectome Project. Neuroimage 80, 105-124.

Greenberg, T., Chase, H.W., Almeida, J.R., Stiffler, R., Zevallos, C.R., Aslam, H.A., Deckersbach, T., Weyandt, S., Cooper, C., Toups, M., *et al.* (2015). Moderation of the Relationship Between Reward Expectancy and Prediction Error-Related Ventral Striatal Reactivity by Anhedonia in Unmedicated Major Depressive Disorder: Findings From the EMBARC Study. Am J Psychiatry 172, 881-891.

Griffanti, L., Salimi-Khorshidi, G., Beckmann, C.F., Auerbach, E.J., Douaud, G., Sexton, C.E., Zsoldos, E., Ebmeier, K.P., Filippini, N., Mackay, C.E., *et al.* (2014). ICA-based artefact removal and accelerated fMRI acquisition for improved resting state network imaging. Neuroimage 95, 232-247.

Hamilton, M. (1967). Development of a rating scale for primary depressive illness. The British journal of social and clinical psychology 6, 278-296.

Jeub, L.G.S., Sporns, O., and Fortunato, S. (2018). Multiresolution Consensus Clustering in Networks. Sci Rep 8, 3259.

Jutla, I.S., Jeub, L.G., and Mucha, P.J. (2011). A generalized Louvain method for community detection implemented in MATLAB. URL http://netwiki amath unc edu/GenLouvain.

MacMahon, M., and Garlaschelli, D. (2013). Community detection for correlation matrices. arXiv preprint arXiv:13111924.

Rush, A.J., Trivedi, M.H., Ibrahim, H.M., Carmody, T.J., Arnow, B., Klein, D.N., Markowitz, J.C., Ninan, P.T., Kornstein, S., Manber, R.*, et al.* (2003). The 16-Item Quick Inventory of Depressive Symptomatology (QIDS), clinician rating (QIDS-C), and self-report (QIDS-SR): a psychometric evaluation in patients with chronic major depression. Biol Psychiatry 54, 573-583.

Salimi-Khorshidi, G., Douaud, G., Beckmann, C.F., Glasser, M.F., Griffanti, L., and Smith, S.M. (2014). Automatic denoising of functional MRI data: combining independent component analysis and hierarchical fusion of classifiers. Neuroimage 90, 449-468.

Schaefer, A., Kong, R., Gordon, E.M., Laumann, T.O., Zuo, X.N., Holmes, A.J., Eickhoff, S.B., and Yeo, B.T.T. (2018). Local-Global Parcellation of the Human Cerebral Cortex from Intrinsic Functional Connectivity MRI. Cereb Cortex 28, 3095-3114.

Scheinost, D., Noble, S., Horien, C., Greene, A.S., Lake, E.M., Salehi, M., Gao, S., Shen, X., O'Connor, D., Barron, D.S.*, et al.* (2019). Ten simple rules for predictive modeling of individual differences in neuroimaging. Neuroimage 193, 35-45.

Shen, X., Finn, E.S., Scheinost, D., Rosenberg, M.D., Chun, M.M., Papademetris, X., and Constable, R.T. (2017). Using connectome-based predictive modeling to predict individual behavior from brain connectivity. Nat Protoc 12, 506-518.

Subelj, L., and Bajec, M. (2011). Unfolding communities in large complex networks: combining defensive and offensive label propagation for core extraction. Phys Rev E Stat Nonlin Soft Matter Phys 83, 036103.

Traud, A.L., Kelsic, E.D., Mucha, P.J., and Porter, M.A. (2011). Comparing community structure to characteristics in online collegiate social networks. SIAM review 53, 526-543.

Trivedi, M.H., McGrath, P.J., Fava, M., Parsey, R.V., Kurian, B.T., Phillips, M.L., Oquendo, M.A., Bruder, G., Pizzagalli, D., Toups, M.*, et al.* (2016). Establishing moderators and biosignatures of antidepressant response in clinical care (EMBARC): Rationale and design. J Psychiatr Res 78, 11-23.

Van Essen, D.C., Smith, S.M., Barch, D.M., Behrens, T.E., Yacoub, E., Ugurbil, K., and Consortium, W.U.-M.H. (2013). The WU-Minn Human Connectome Project: an overview. Neuroimage 80, 62-79.

Yeo, B.T., Krienen, F.M., Sepulcre, J., Sabuncu, M.R., Lashkari, D., Hollinshead, M., Roffman, J.L., Smoller, J.W., Zollei, L., Polimeni, J.R.*, et al.* (2011). The organization of the human cerebral cortex estimated by intrinsic functional connectivity. J Neurophysiol 106, 1125-1165.